Personnel staffing and scheduling during disease outbreaks: A contact network-based analysis

Ana Batista[a,b,*], Abhishek Senapati[a,b], Mansoor Davoodi[a,b], Justin M. Calabrese[a,b,c]

[a] *Helmholtz-Zentrum Dresden-Rossendorf (HZDR), Dresden, Germany*
[b] *Center for Advanced Systems Understanding (CASUS), Görlitz, Germany*
[c] *Dept. of Biology, University of Maryland, College Park*

Abstract

Personnel scheduling in organizations can be disrupted by unforeseen events that require efficient planning. A recent example is the COVID-19 pandemic that disrupted global operations, compromising people's health and safety. Many organizations were forced to transition to full remote work to prevent the spread of the virus and ensure employee safety. Although working entirely remotely is effective for some organizations, others must balance workplace occupancy and infection risk to keep their operations functioning efficiently despite a global health crisis. We address this issue by developing a days-off scheduling model that captures employees' interactions through the underlying contact network. To solve the problem, we propose a Mixed Integer Linear Programming model considering a Microscopic Markov Chain Approach to determine the probability of infection in a contact network that mimics the employees' interactions. The model determines, during a given planning period, the optimal staffing mix to maximize occupancy while minimizing the risk of infection in the presence of testing protocols. We conduct sensitivity analysis to assess the approach's robustness while considering different contact networks and testing strategies. Through extensive computational analysis, we show that the degree of contact among employees is not the sole factor to consider when defining personnel scheduling policies during disease outbreaks. The decision-maker must balance the employee allocation with tailored testing interventions based on management's priorities to mitigate the effects while ensuring the desired occupancy at a lower risk.

Keywords: `personnel scheduling, days-off scheduling, disease modeling, COVID-19`

1. Introduction

The Personnel Scheduling Problem (PSP) aims to allocate employees to tasks and shifts to meet organizational needs, staff preferences, and service demands. Organizations typically aim to effectively plan their human resources to fulfill service levels at the minimum cost Ernst et al. (2004b). Workforce planning can be affected by external

*Corresponding author
Email addresses: `a.batista-german@hzdr.de` (Ana Batista), `a.senapati@hzdr.de` (Abhishek Senapati), `davood68@hzdr.de` (Mansoor Davoodi), `j.calabrese@hzdr.de` (Justin M. Calabrese)

(unpredictable) events that cause disruptions in performance and regular operations, such as natural disasters, man-made disasters, and disease outbreaks, to mention a few (Ernst et al., 2004a; Rachaniotis et al., 2012). A recent example of a disruptive event that heavily affected workforce planning is the coronavirus disease 2019 (COVID-19) pandemic. To prevent the spread of the virus early in the pandemic, the World Health Organization (WHO) recommended many non-pharmaceutical measures, including the use of protective masks, social distancing, and nationwide lockdowns (WHO COVID-19, 2020). Along with these measures, several organizations were forced to resort to a full remote work to prevent the disease transmission and ensure safety in the workplace (Harapan et al., 2020; Rawson et al., 2020). However, due to technological limitations or the nature of their operations, not all companies e.g., in the service sector, retail, healthcare, manufacturing) can implement such a strategy, not to mention the social and economic costs that these policies entail. To date, little is known about balancing workplace occupancy and the risk of infection in these organizations while keeping operations ongoing. Therefore, deriving optimal occupancy policies in the context of disruptive events such as a pandemic is crucial for workforce planning to control the spread of the virus and its impact on regular operations.

The spread of some infectious diseases such as the Severe Acute Respiratory Syndrome Coronavirus 2 (SARS-CoV-2) that caused the COVID-19 pandemic is generally driven by close contact among the individuals (Block et al., 2020; Li et al., 2020; Shereen et al., 2020; Harapan et al., 2020). Since the number of contacts among employees increases with workplace occupancy, the most practical policy to control viral spread is to limit such interactions, in addition to complementary measures such as regular testing, vaccination, and the use of masks. Within a high risk environment that compromises people's lives, the challenge is to find the optimal mix of different types of employees that guarantees the expected service levels at the minimum risk of infection. In this context, the days-off scheduling problem (See Ernst et al. (2004b) for a review on this problem) can be employed to determine the optimal number of days employees can be present at the workplace while minimizing the risk of infection. The days on/off in the scheduling plan refer to a flexible allocation approach that allows employees to work both in the workplace and remotely. Then, to measure the risk of infection in the workplace, the days-off scheduling plan must be integrated with a disease transmission model that computes the virus spread over the planning horizon according to the employees' interactions.

Employee interaction is one of the most important aspects of preventing the virus from spreading in the workplace. Understanding the role of interactions in disease spread is difficult due to the complexity of determining its different components such as the type and duration of the contacts. The interactions is often represented by a network in which nodes denote the individuals, and edges capture the connections between them (Kiss et al., 2017). The study of networks has its origins in graph theory, e.g., (Bollobás, 2012), which focuses on studying the network capabilities. In epidemiology, on the other hand, the main goal is to study the spread of a disease considering the network as a constraining background (Keeling & Eames, 2005b). This approach facilitates the representation of real contact patterns and the analysis of the evolution of the disease over time. The network (graph) structure provides valuable insights into the interaction patterns and their effect on disease transmission. Keeling & Eames (2005a)

explored the influence of network structures on epidemic dynamics and showed that specific properties of a network structure, such as heterogeneity in the degree distribution, and clustering, significantly impact the disease dynamics. For instance, random networks are characterized by a random distribution of connections, lack of clustering, homogeneity of connections, and short path lengths (Newman et al., 2002; Boccaletti et al., 2006). In contrast, scale-free networks (Barabási & Albert, 1999) present a higher heterogeneity of connections following the power law distribution so that a few individuals have significantly more connections than the rest. Other common networks that represent social network structures are, Lattices, and Small-world, differing in clustering, degree distribution, and average path length. Overall, networks with short path lengths and little clustering have the quickest epidemic growth rate based on the number of contacts per individual (See Keeling & Eames (2005b) for a review of infectious diseases through contact networks). There exist several theoretical approaches to study the contagion dynamics in a complex network; namely, mean-field (MF), heterogeneous mean field (HMF), quenched mean-field (QMF), dynamic message passing approach (DMP), and microscopic Markov chain approach (MMCA) (See Wang et al. (2017) for a detailed review). Some approaches deal with the aggregated dynamics of the nodes (MF) or class of nodes based on their degree (HMF). On the other hand, approaches like QMF, MMCA, and DMP capture the dynamics at the level of single nodes. In this study, we consider an MMCA (Gómez et al., 2010; Gómez-Gardeñes et al., 2015), a comparatively less computationally intensive discrete time individual node-based approach to study the underlying disease dynamics in a network.

Inspired by the recent events of the COVID-19 pandemic, this study provides a novel approach to the PSP under disruptive events. The approach aims to satisfy daily labor demands at the minimum infection risk. We propose a Mixed Integer Linear Programming (MILP) model to solve a days-off scheduling model by determining the optimal staffing mix to be allocated while taking into account the effect of interaction among staff in a contact network-based approach, the probability of infection transmission of the staff that works in close contact, and interventions such as vaccination and testing. To the best of our knowledge, this is the first study to explore the PSP employing a network-based epidemiological model using a formal optimization approach to balance workplace occupancy, workload demand coverage, and risk of infection.

The remainder of this paper is organized as follows. Section 2 presents the state of the art of the PSP during under disruptions, infectious disease modeling on networks and the main contributions of the study. Section 3 describes the problem under study, the mathematical notation, the main assumptions, and performance metrics. Section 4 presents the case study of the days-off scheduling model and describes the computational experiments and results. Section 5 analyzes the proposed model through sensitivity analysis to explore how variations in key parameters affect the optimal solution. Finally Section 6 summarizes the main findings of the study.

2. State of the art

In this section, we present the state of the art in two complementary research lines related to this study: personnel scheduling under disruptive events and infectious disease modeling on networks.

2.1. Personnel scheduling under disruptions

The personnel scheduling problem (PSP) is known to be a challenging problem (Brucker et al., 2011), and consequently, due to its practical relevance, it has been widely studied in the literature Baker (1976); Ernst et al. (2004a,b); Van den Bergh et al. (2013); Qin et al. (2015); Özder et al. (2020). According to Baker (1976), the PSP is classified into shift scheduling, days-off scheduling, and tour scheduling problems. Shift scheduling problems aim to determine which shifts to perform as well as the number of staff that must be assigned to each shift to meet demand requirements. Days-off scheduling problems include rest days between work days, typically considered for flexible shift scheduling. Finally, tour scheduling problems combine the shift and days-off scheduling problems, considering more than one shift in a day; it determines staff allocation per hour and days of the week. Relevant to this study is the days-off scheduling problem to determine the optimal size and mix of a workforce to balance the risk of infection and workplace occupancy in the time horizon.

The PSP has received little attention in the literature when it comes to emergencies or disruptive events (Ernst et al., 2004a). The specific case of staff scheduling in pandemic situations is an emerging topic that has gained attention with the start of the COVID-19 pandemic. The healthcare system has been one of the most affected sectors during the pandemic in personnel scheduling. Specialized hospital workers are a limited resource that cannot be rapidly replaced. Due to the close contact with infected patients, doctors and nurses get exposed, causing a shortage in staff availability and scheduling disruptions. A study by Güler & Geçici (2020) proposed a Mixed Integer Programming (MIP) model to balance the medical staff workload in COVID-19 dedicated departments while guaranteeing the physician's safety. Similarly, Musliu & Winter developed a real-world problem applied to a hospital in Austria. They developed a constraint programming model for physician rostering during the pandemic. To minimize the interactions among the staff in case of an infection, they proposed a set of constraints that efficiently partition the staff into different departments. Seccia (2020) studied the nurse rostering problem during emergency situations. The authors proposed a model to balance nurse workload and allow flexibility under limited personnel availability. Other studies have focused on developing strategies to mitigate the spread of the virus among healthcare workers in hospitals. These studies employ compartmental models to explore strategies such as weekly alternating the staff (Sánchez-Taltavull et al., 2021), regular testing, and desynchronization protocols (Sanchez-Taltavull et al., 2021), and cyclic schedules (Karin et al.).

For the logistic sector, Zucchi et al. (2021) proposed a real-life PSP applied to a pharmaceutical warehouse in Italy. The authors proposed a MILP to minimize the deviations between the staff's weekly contractual hours and the actual allocated hours. The staff is allocated into separate groups to prevent the spread of the virus. In order

to assess the contagion risk resulting from the schedule, the authors defined a risk factor based on a network graph configuration. The solutions of the proposed schedule outperform the actual practice in the company. Guerriero & Guido (2021) developed a tour scheduling problem applied to an Italian university to ensure employee satisfaction and safety in the workplace. The study considers employee availability and allocation preferences (i.e., working remotely) by adding an intermediate shift to the regular morning - afternoon shifts. By employing real data, the authors provided a better performance compared to the schedules done manually. The pandemic has affected the construction sector as well. The staff must comply with social distancing measures to prevent the spread of the virus, delaying the completion of projects. In this regard, Aslan & Türkakın (2021) proposed a resource constrained project scheduling model employing a multi-objective genetic algorithm to minimize project duration, project cost, and staff infection risk. The authors test several configurations of worker labor limits (e.g., total worker allowance, individual activity requirements) and provide a set of optimal solutions according to decision-maker priorities. Testing strategies have also been studied as a means to mitigate the spread of the virus in organizations. For instance, Davoodi et al. (2022) proposed a staffing model to study the trade-off between workplace occupancy and productivity and its effect on the risk of infection in the workplace. The risk of infection is computed considering an aggregated probabilistic framework that disregards the possibility of tracking infection status at an individual level. More general studies (D'angelo et al., 2021; Rawson et al., 2020; Mauras et al., 2021; Abdin et al., 2021) have focused on studying strategies for reopening activities during a pandemic, but these studies lack the specifics of personnel scheduling in organizations.

Although some of the studies mentioned above have looked into the emerging topic of personnel scheduling during a pandemic, no existing study, to our knowledge, has explored the PSP considering a contact network-based approach for disease progression analysis using formal optimization methods. See Jordan et al. (2021); Choi (2021) for a comprehensive review on Optimization in the context of the COVID-19 pandemic.

2.2. Infectious disease modeling on networks

Many epidemiological models have been proposed to study the spread of a virus during an epidemic. Mathematical modeling of infectious diseases can be classified into two broad classes: statistical and mechanistic models. Statistical models are data-driven methods generally used to forecast the progression of a disease, including Bayesian techniques and deep learning methods. On the other hand, mechanistic models are employed to gain better understanding on the mechanism of disease spread in a population, includes compartmental models (e.g., SIR (Susceptible, Infectious Removed, and variants) and agent-based network models. The main limitation of compartmental-based modeling is the assumption that the population under consideration is homogeneously mixed. This assumption limits the possibility of exploring more realistic situations where heterogeneity in various factors such as contacts, infectiousness, and level of personal protection of the individuals is expected.

This issue can be avoided if we consider the MMCA modeling framework, where instead of studying aggregated dynamics, it enables us to zoom into the dynamics of each node individually. The MMCA was first formulated

in studying contact-based epidemics spreading on complex networks by Gómez et al. (2010). Later this modeling framework has been used to investigate a range of theoretical aspects of epidemic spreading, such as threshold-based behavior of epidemic spreading (Larremore et al., 2011; Valdano et al., 2015), the occurrence of first order transitions due to reinfection (Gómez-Gardeñes et al., 2015), the interplay between awareness and epidemic spreading in multiplex networks (Granell et al., 2013, 2014; Wang et al., 2019), and abrupt phase transitions in higher-order interaction networks (Matamalas et al., 2020). Recently, a few mathematical models have been developed based on this modeling framework to study the transmission dynamics of the COVID-19 pandemic. For instance, Arenas et al. (2020) investigated the impact of mobility and social distancing interventions on COVID-19 dynamics in Spain. Another study (Hazarie et al., 2021) used this modeling framework to explain the heterogeneity in the COVID-19 spreading process across 133 cities in the United States.

Limited works have considered formal optimization methods in the context of network-based epidemiological models. Of particular interest is the work of Bagger et al. (2022), which developed an optimization model for reducing disease spread in activities (e.g., shopping, school teaching, theater events, sports activities) employing a macroscopic agent-based approach with an SEIR model. The model considers a network graph representation of the participants' interactions to assess the structures that reduce the spread of diseases. They found that the disease spread can be controlled by not only considering the size of the activity but limiting the number of contacts among the individuals. However, Baggers' study focuses on country-level initiatives rather than specific organizations; it disregards the specifics of personnel scheduling, such as the days-off scheduling problem through contact network analysis that we cover in this study.

The contribution of this study is twofold. First, we study the PSP under disruptive events such as a pandemic, considering a network-based epidemiological model. We consider an MMCA to determine the probability of infection in a contact network based on the employees' interactions and interventions, including testing, vaccination, and personal protection. We develop an MILP model to solve a days-off scheduling problem that maximizes workplace occupancy while guaranteeing the minimum risk of infection and ensuring workload demand coverage. Second, we perform extensive computational studies that demonstrate the capabilities of the proposed model to optimally balance workplace occupancy, risk of infection (to a certain extent), and workload demand coverage. We highlight the importance of developing optimal workforce planning under disruptive events (e.g., a pandemic) to achieve staffing levels while providing safety in the workplace. The approach can be used as a tool to schedule personnel during a disease outbreak in real-world organizations.

3. Description of the problem

In this section, we present the proposed solution framework to solve the PSP in the context of disruptive events such as disease outbreaks. We first characterize and describe the problem and main assumptions in Subsection 3.1. Then, in Subsection 3.2, we present the MMCA used to determine the probability of infection in a contact network

based on the employee's interactions. Finally, in Subsection 3.3, we describe the MILP formulation coupled with the MMCA and performance metrics in Subsection 3.4.

3.1. Problem definition

The personnel scheduling problem in this study arises in the context of the COVID-19 pandemic. In the workplace, the employees are in close contact, which increases the risk of infection transmission. Thus, to mitigate the propagation of the virus, the managers have to determine effective policies that control the spread of the virus while guaranteeing the expected service levels of workload demand coverage. These organizations have the flexibility of a working hybrid mode, where employees can work remotely or on-site; however, a number of employees must be present in the workplace to guarantee the accomplishment of staffing measures. Weekly, the manager has to determine the optimal workforce size in the workplace by deciding which employee to allocate on-site, the day of allocation, and for how many days to allocate them. This problem is a special case of the days-off scheduling problem considering consecutive days of allocation. The employees differ according to the probability of transmission (i.e., vaccination status, age) and priority of allocation in the time horizon. In addition, to define the workforce schedule, the managers need to consider safety measures to keep the risk of infection to a minimum, such as wearing masks, social distancing by limiting workplace occupancy, and regular testing.

The goal of this study is to find a balance between workplace occupancy, infection risk, and workload demand coverage by taking into account the probability of infection transmission, the effect of interaction among the employees who are in contact with each other, and interventions such as testing, vaccination, and personal protection. In summary, the decisions to make are: (i) Which employee type to allocate in the time horizon; (ii) When to allocate the employee according to capacity availability; (iii) For how many consecutive days to allocate the employees, and (iv) How many infected employees result from the allocation. The required notation used in the proposed model are listed below.

Nomenclature

Sets and subsets

T	Set of periods, indexed by t.
E	Set of employees, indexed by i.
S	Set of employees types, indexed by s.
E_s	Subset of employees who belong to the type, s, $E_s \subseteq E$.
$\text{LINKS}_{E \cap E}$	Subset of employees in contact, indexed by (i, j), $E \cap E$.

Parameters

n	Total number of employees.
β_s	Probability of transmission per employee type s.
τ_s	Probability of testing for employee type s.
pi_i^0	Probability of infection of employee i at time $t = 0$.
σ	Sensitivity of the test.
pq_i^0	Quarantined employees i at time $t = 0$.
A_{ij}	Contact network of employees $(ij) \in \text{LINKS}$.
r_{is}	Number of employees i type s required

(workload demand).

L_{is} Number of consecutive days to allocate employee i type s.

ω_t Maximum capacity availability to allocate at time t.

α Threshold on the expected number of infections allowed per day.

$u^{\max}$ Upper bound on the total maximum allocation days to discount.

w_i Allocation priority per employee i.

c_i^{OC} Penalty weight associated with the discounted days of allocation per employee i.

c^{IF} Penalty weight associated with the surplus of infections allowed.

Decision Variables

pi_{it} Probability of infection of employee i at time $t > 0$.

pq_{it} Probability of quarantined employees i at time $t > 0$.

X_{ist} Binary variable denoting the allocation of employee i type s in period t.

Y_{ist} Binary variable denoting the initiation of the allocation of employee i type s in period t.

Γ Slack variable on the number of infected employees.

Δ_{is} Slack variable on the discounted allocation days per employee i type s.

The main assumptions considered in the personnel scheduling model are described as follow:

1. The time horizon is discretized and divided into several time slots of equal size, typically a day.
2. The scheduling decisions are made at the beginning of the period for the entire planning horizon.
3. The days-off scheduling problem assumes a 7-day working week with flexible on-off days of allocation for the employees. Hence, we consider a fixed shift length of continuous working hours.
4. The required employees in the time horizon, κ_{is}, (i.e., workload demand) is known and specified by the decision-maker.
5. The allocation days per employee, L_{is}, refers to the required time to be present in the workplace. We assume that L_{is} is continuous and uninterruptible. This assumption have been demonstrated as an efficient scheduling strategy during disease outbreaks (Sánchez-Taltavull et al., 2021; Ely et al., 2021; Lim et al., 2020). Thus, the employee is always assigned for the total duration at the beginning of a time slot. As a result, the allocation can end at any time, not only at the end of a time slot.
6. The available capacity, ω_t, is known at the beginning of the planning period and is time-varying on the planning horizon. The capacity availability is considered variable due to workplace restrictions on social distancing and area blockage that may vary over the planning horizon.
7. Understaffing (on-site) is allowed due to capacity limitations and infection prevention risk. We assume that the organization offers flexibility for remote working to the employees. Thus, the non-allocated employees are assumed to be working from home.

8. The test, τ_s, refers to the probability of testing employees in the time horizon. We assume that employees that test positive are immediately placed in quarantine (i.e., the employee will be absent from the workplace).

9. The probability of transmission, β_s, per employee type s is known. We classify the employees according to their viral load and emission rates. For instance, some of them can emit more viruses than others according to the immune system of the individual, age, and vaccination status.

10. The initial probability of infection, pi^0, per employee i at $t = 0$ is considered as random. pi^0 can be translated as the probability of the employee getting infected during a rest day or holiday.

11. The probability of quarantined employees, i at $t = 0$, pq^0, is considered 0. Thus, we assume that at the beginning of the time horizon, there are no "tested" individuals.

3.2. Modeling the probability of infection in a contact network (MMCA)

In this MMCA modeling framework, we consider n employees whose interaction is defined by the underlying adjacency matrix $A = (A_{ij})$, where $A_{ij} = 1$ if node i and node j has a connection and $A_{ij} = 0$ if they do not have any connection. At each time step, t, for each node i, we calculate two probabilities $p_{i,t}$ and $q_{i,t}$ which denote the probability of being infected and probability of being quarantined, respectively. Here, we assume that quarantining is the consequence of positive results in testing. The node i remains infected at a particular time step if it was infected in the previous time step and was not tested. On the other hand, it remains quarantined if in the previous time step it was in quarantine or it was infected and subsequently tested. The time evolution probabilities of being in a particular state (i.e., infected and quarantined) is given by the following discrete time model:

$$\begin{aligned} p_{i,t+1} &= \sigma\Big(1-\tau\Big)p_{i,t} + \Big(1 - p_{it} - q_{it}\Big)\left[1 - \prod_{j=1}^{n}(1 - \beta A_{ij}p_{jt})\right] \\ q_{i,t+1} &= \sigma\tau p_{it} + q_{it}, \end{aligned} \tag{1}$$

where β denotes the probability that after each contact with an infected node the disease will transmit to the susceptible node, τ denotes the probability that the infected node will be tested, and σ refers to the sensitivity of the test.

3.3. The personnel scheduling problem formulation

The MILP formulation for the personnel scheduling problem during disease outbreaks is described in Equations (2)–(15). In order to characterize a system in which the employees are allocated over the planning horizon without interruptions, we consider a set of constraints for uninterruptible services (Batista et al., 2020). To compute the risk of infection, we extended the MMCA model presented in Equation (1) by including the set, S to categorize the employees according to its disease transmission, β_s and testing rate, τ_s.

$$\max_{\mathbf{X},\mathbf{Y},\boldsymbol{\Delta},\boldsymbol{\Gamma}} \sum_{s=1}^{S}\sum_{i=1}^{E_s}\sum_{t=1}^{T} Y_{ist} w_i - \sum_{i=1}^{E}\sum_{s=1}^{S} \Delta_{is} c_i^{\mathrm{OC}} - \Gamma c^{\mathrm{IF}} \tag{2}$$

(a) (b) (c)

s.t.:

$$pi_{i,t+1} = \sigma\Big(1-\tau_s\Big)pi_{it} + \Big(1 - pi_{it} - pq_{it}\Big)\left[1 - \prod_{j=1}^{n}(1-\beta_s A_{ij} pi_{jt})\right] \qquad \forall s \in S, i \in E_s, t = 1,\ldots,T \tag{3}$$

$$pi_{it} = pi_i^0 \qquad \forall i \in E, t = 0 \tag{4}$$

$$pq_{i,t+1} = \sigma\tau_s pi_{it} + pq_{it} \qquad \forall s \in S, i \in E_s, t = 1,\ldots,T \tag{5}$$

$$pq_{it} = pq^0 \qquad \forall i \in E, t = 0 \tag{6}$$

$$\frac{1}{T}\sum_{i=1}^{E}\sum_{s=1}^{S}\sum_{t=1}^{T} pi_{it} X_{ist} \le \alpha + \Gamma \tag{7}$$

$$Y_{ist} \ge X_{ist} - X_{ist-1} \qquad \forall a \in S, i \in E_s, t = 1,\ldots,T \tag{8}$$

$$Y_{ist} \ge X_{ist} \qquad \forall s \in S, i \in E_s, t = 0 \tag{9}$$

$$\sum_{t=1}^{T} Y_{ist} \le 1 \qquad \forall s \in S, i \in E_s \tag{10}$$

$$\sum_{t=1}^{T} Y_{ist} L_{is} \le \sum_{t=1}^{T} X_{ist} + \Delta_{is} \qquad \forall s \in S, i \in E_s \tag{11}$$

$$\sum_{a=1}^{S}\sum_{i=1}^{E_S} \Delta_{is} \le u^{\max} \tag{12}$$

$$\sum_{t=1}^{T} Y_{ist} \le r_{is} \qquad \forall s \in S, i \in E_s \tag{13}$$

$$\sum_{i=1}^{E}\sum_{s=1}^{S} X_{ist} \le \omega_t \qquad \forall t \in T \tag{14}$$

$$X_{ist} \in \{0,1\},\ Y_{ist} \in [0,1], \Delta_{is} \ge 0, \Gamma \ge 0 \qquad \forall i \in E, s \in S, t \in T \tag{15}$$

The objective function, (2), aims to maximize the total benefit of the scheduling plan, which consists of three terms: the first term refers to the (a) weighted benefit of employee allocation; the second term (b) penalizes the discounted days of allocation per employee type; the third term (c) penalizes the additional infected employees from the defined threshold. The proposed model must satisfy a set of constraints. Constraint (3)–(6) computes the probability of infection by means of a forward procedure as explained in Section 3.2. By considering the matrix $\mathbf{A}$, we estimate the probability of node i being infected at time t. The probability of infection depends on the network structure and the testing rate, τ_s. Constraint (7) guarantees that the number of infected personnel allocated does not exceed a defined

threshold, α. The slack variable Γ adds flexibility to the allocation process, by allowing a surplus in the number of infections over the defined threshold value. Constraint (8) and (9) guarantees the continuity of allocation during the defined period, L_{is}. Constraint (10) indicates that an employee must be allocated at most once in the time horizon. Note that with constraint (10) we allow understaffing (on-site); the employees not allocated are assumed to work remotely. Constraint (11) guarantees that there are enough time slots to allocate the duration of the employee schedule, L_{is}. The slack variable, Δ_{is}, captures the variation in the allocated days. Constraint (12) introduces a limit on the maximum days to discount from the employee schedule allocation. Constraint (13) accounts for demand fulfillment in the time horizon. Constraint (14) imposes capacity availability limitations in the planning horizon. Finally, constraint (15) defines the variables' domain.

3.4. Performance metrics

To assess the viability of the proposed approach, we defined several performance metrics. These metrics allow us to evaluate the impact of personnel scheduling allocation on workplace infection risk. A detailed definition of the metrics is given as follows:

1. *Risk of infection on employee allocation*: Measures the expected number of infected employees resulting from the employee allocation.

$$RI = \frac{1}{T} \sum_{s=1}^{S} \sum_{i}^{E_s} \sum_{t=1}^{T} X_{ist} pi_{it} \tag{16}$$

2. *Weekly demand coverage*: Measures the percentage of workload demand covered by employee type s.

$$\%DC = \frac{\sum_{i=1}^{E} \sum_{t=1}^{T} Y_{ist}}{\sum_{i=1}^{E} r_{is}} \cdot 100 \quad \forall s \in S \tag{17}$$

3. *Maximum budget of reduced days of allocation*: Measures the percentage of days removed from the requested, L_{is}.

$$\%DA = \frac{\sum_{s=1}^{S} \sum_{i=1}^{E_s} \Delta_{is}}{u^{\max}} \cdot 100 \tag{18}$$

4. *Average allocated days*: Measures the average number of days allocated per employee.

$$AL = \frac{\sum_{i=1}^{E}\sum_{e=1}^{S}\sum_{t=1}^{T} X_{ist}}{\sum_{i=1}^{E}\sum_{e=1}^{S}\sum_{t=1}^{T} Y_{ist}} \tag{19}$$

5. *Occupancy level*: Measures the expected occupancy in a weekly planning horizon.

$$\%OCC = \frac{1}{T}\frac{\sum_{i=1}^{E}\sum_{s=1}^{S}\sum_{t=1}^{T} X_{ist}}{\omega_t} \cdot 100 \tag{20}$$

6. *Total benefit of the scheduling plan*: Measures the total benefit of allocation gained in a weekly planning horizon.

$$\kappa = \sum_{s=1}^{S}\sum_{i=1}^{E_s}\sum_{t=1}^{T} Y_{ist} w_s - \sum_{i=1}^{E}\sum_{s=1}^{S} \Delta_{is} c_i^{\mathrm{OC}} - \Gamma c^{\mathrm{IF}} \tag{21}$$

4. Computational experiments and results

In this section, we present the data, experiments, and discussions conducted to assess the optimal balance between workplace occupancy, risk of infection, and demand coverage when solving the proposed PSP. We study the impact of disease spread on staffing decisions, considering a network-based epidemiological approach. We first describe the input setting and case study defined to solve the days-off scheduling model in Subsection 4.1. Then in Subsection 4.2 we present and analyze the base case study in terms of the scheduling and allocation decisions and performance metrics. The model was implemented on an Intel i7, 3GHz with 32 GB of RAM using CPLEX 12.7.0, with an optimality gap set to zero.

4.1. Case study and data description

The case study considered in this paper is inspired by the recent COVID-19 pandemic. The input data and scenarios correspond to the data reported related to the SARS-CoV-2 virus. To assess the effectiveness of the proposed approach, we have defined a base case study considering the assumptions described in Subsection 3.1. The model can be applied to any organization that considers workforce flexibility in the scheduling process so that the employees can work on-site or remotely to perform their daily tasks. To solve the suggested days-off scheduling model, we use synthetic data. For the base case, we consider a discretized time horizon of $T = 7$ days for a weekly schedule plan. During the defined time horizon, $n = 100$, employees have to be allocated, which are classified into three main categories, $S = 3$.

The probability of disease transmission of employees, β, varies among the employees categories defined as, s_1 low risk, s_2 medium risk, and s_3 high risk. Different risk groups can be defined based on the age of the employee, vaccination status (i.e., whether fully vaccinated or not), and level of personal protection in the office. For defining β, we consider an initial value from a set of scenarios as reported in Lelieveld et al. (2020) for office environment infection risk. The baseline value corresponds to employees in category, $s = 3$, where $\beta_3 = 0.12$[1]. For the other categories we set $\beta_2 = (1 - 0.30)\beta_3$ and $\beta_1 = (1 - 0.5)\beta_3$, which implies 30% and 50% immunity, for medium and low risk categories respectively. Here we assume that for the medium and low risk groups, the probability of disease transmission is reduced by 30% and 50% compared to the base case. We consider the probability of testing, $\tau_s = 0.20$ for all patient categories. The sensitivity of the test (rapid antigen test) is set to $\sigma = 90\%$ (CubasAtienzar et al., 2021).

Employee category	Employee required	Probability of disease transmission	Test probability	Description
s	r_{is}	β	τ	
1	25	0.060	0.20	Low risk
2	45	0.084	0.20	Medium risk
3	30	0.120	0.20	High risk

Table 1: Base case days-off scheduling model data description.

We define the initial condition ($t = 0$) of the probability of infection, pi_i^0, considering a random uniform distributed [0, 1] per employee i. This value can be interpreted as the probability of an employee introducing the infection to the workplace. Note that the setting of pi^0 depends on several preventive policies imposed by the local health authorities and their implementation. In the case of the preventive measures strictly followed by the employees, we can argue that the initial risk (getting infected during rest day/holiday/working from home) is lower than the risk of getting infected in the workplace due to interactions via the contact network. On the contrary, such social distancing measures are easier to implement and follow in the workplace. Thus, without loss of generality, we have defined this value as a random parameter. The initial condition ($t = 0$) for the probability of quarantined employees, pq_i^0, is set to $pq_i^0 = 0$. So, we consider that there are no quarantined employees at the start of the scheduling plan. The interactions among employees are defined according to a known undirected graph defined by the adjacency matrix, $\mathbf{A}$, that summarizes the connections of the employees within the network.We employ a Barabasi-Albert (BA) scale-free network for the base case, which follows the power-law degree distribution. Scale-free networks are commonly used to mimic the interactions where heterogeneity in connection is present. In organizations, employees usually have heterogeneous interactions; for instance, most employees have a moderate number of contacts, whereas few have a very high number of contacts due to the nature of their work responsibilities[2].

[1]This value can be regarded as the situation where variants of SARS-CoV-2 with high transmissibility like *Omicron* is dominant Lyngse et al. (2021); World Health Organization and others (2022).

[2]An extended description of the network measures, average degree distribution, $\overline{dg}$, average clustering coefficient, $\overline{C}$, and average path length,

The total number of employees required, r_{is}, in the time horizon (i.e., workload demand) is distributed among the three employee categories. For the base case, which accounts for, $n = 100$ employees, the workload demand is distributed as follows: $s_1 = [25\%]$; $s_2 = [45\%]$, and $s_3 = [30\%]$. Note that this distribution may vary according to organization status during the scheduling plan definition. Table 1 summarizes the setting parameters for the number of employee required, probability of infection, and test interval per employee category. We defined the number of consecutive days to allocate an employee, L_{is}, considering a uniform distribution, so that $L_{is} \in [2, 5]$, for all employees, disregarding their category. The capacity availability, ω_t, imposes a limit on the number of allocated employees in each period t. This parameter is defined to comply with social distancing regulations in the workplace, so it varies over time to $[50 - 75]\%$ of daily occupancy. The threshold on the number of infections allowed, α, corresponds to the expected number of infected employees allowed per day. The threshold value must be defined by the decision-maker to balance occupancy in the workplace; for the base case, we have set it to 8% of the total number of employees. The upper bound on the total maximum allocation days to decrease, $u^{\max}$, is set to 30, which refers to the maximum number of days that can be subtracted from the preferred days, L_{is} among all allocated employees. This value depends on the decision maker's willingness to allow the employees to be allocated in the workplace for fewer days than planned.

The objective function of the proposed model concerns two costs related to the penalty for decreasing days of allocation from the preferred days, c_i^{OC}, and a penalty cost associated with the additional infections that surpass the defined threshold, c^{IF}. We also consider the weight, w_i, related to allocation priority (benefit) per employee i. To define the weights of the model, we consider a lexicographic weighting rule, commonly used in multi-objective optimization (Cohon, 2004). This method lets decision-makers easily define a weighting scheme based on a preferred priority. In addition, in the optimization process, what matters is the proportion among the weights rather than the value itself. We set $w_i \gg c^{\text{IF}} \gg c_i^{\text{OC}}$ so that allocating the maximum number of employees while keeping safety in the workplace is the primary goal while still aiming at assigning personnel as many consecutive days as the daily capacity availability allows.

4.2. Days-off scheduling model: Contact network based-analysis

In this section, we assess the proposed days-off scheduling model considering the performance metrics described in Section 3.4. We analyze the solutions by answering the questions, when and which employee to allocate, and for how many consecutive days in the planning horizon. We answer these questions considering the threshold definition (expected number of infected employees), capacity availability, and the effect of the contact network characteristics on the scheduling and allocation decisions. We evaluate three strategies: Full allocation, Partial allocation, and Days-off allocation. The Full allocation strategy refers to the assignment of employees by relaxing Constraints (7), which limits the number of infected employees with the threshold value, α, and (14) that constrains the capacity availability so that there is no imposition of social distancing in the workplace. The Partial allocation strategy allocates employees

$\bar{k}$, is presented in Appendix A.

partially, according to the capacity availability, so in this strategy, only Constraint (7) is relaxed. Finally, the days-off strategy allocates the employees imposing constraints on the expected number of infected employees and capacity availability to maximize occupancy in the workplace at the minimum risk of infection.

To simulate a pandemic transmission process in the workplace, we generate three contact networks, considering a BA scale-free network, commonly presented in social interactions. Figure 1 shows the underlying networks of connections that have been constructed based on synthetic data. The contact networks differ by the average degree distribution, $\overline{dg}$ that characterizes the average number of edges attached to each node and the degree of connection among the staff. We identify the contact networks as N1 : $\overline{dg} = 3.92$; N2 : $\overline{dg} = 18.00$, and N3 : $\overline{dg} = 32.00$. Note that for a higher value of the average degree distribution ($\overline{dg}$), the average clustering coefficient ($\overline{C}$) and average path length ($\bar{k}$) also vary, which would result in different disease transmission routes in the contact network. Ideally, an organization should impose social distance restrictions in the workplace to limit the number of interactions among workers (e.g., limiting in-person meetings and large groups gatherings), so a high value of $\overline{dg}$ may indicate a low level of adherence to the protocols and policies in the organization.

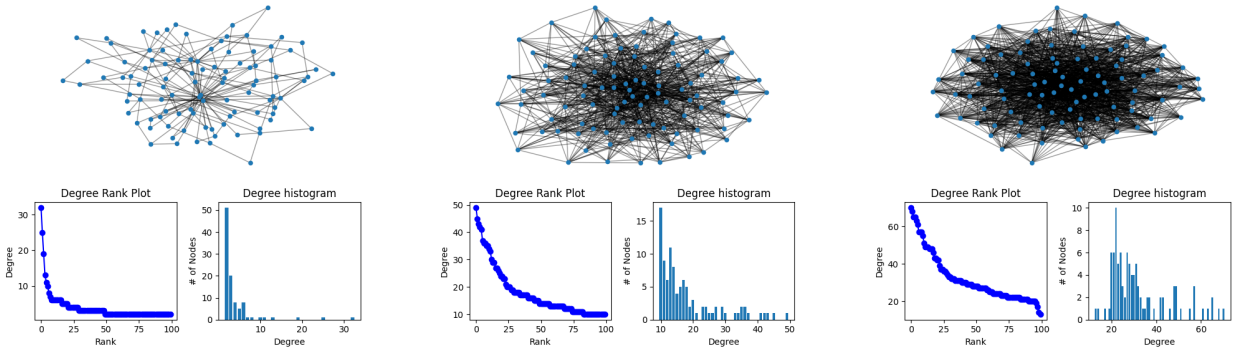

(a) N1 (b) N2 (c) N3

Figure 1: Barabasi-Albert Scale-free contact networks simulating the social interactions in an organization, $n = 100$ nodes. **Characteristics**: Figure 1a: $\overline{dg} = 3.92$; $\overline{C} = 0.18$; $\bar{k} = 2.86$. Figure 1b: $\overline{dg} = 18.00$; $\overline{C} = 0.28$; $\bar{k} = 1.86$. Figure 1c: $\overline{dg} = 32.00$; $\overline{C} = 0.41$; $\bar{k} = 1.68$.

Figure 2 presents the solution of the proposed approach for the base case study[3]. The left panel presents infection curves for the assessed strategies: Full allocation, Partial allocation, and Days-off allocation. Each graph shows the results for the three networks structures (N1, N2, N3) differing by $\overline{dg}$, $\overline{C}$, and $\bar{k}$. The right panel shows the weekly allocation plan for the employee categories and network structures. The solutions correspond to the Days-off allocation strategy. In Table 2 we summarize the performance metrics that answer the key questions in this study, whom to allocate, for how many consecutive days, and when to allocate.

Several observations can be drawn from the computational experiments and the results provided in Table 2. First, in the left panel of Figure 2, we observe that the days-off allocation strategy results in better performance regarding

[3]Extended numerical results can be found in Appendix B, Tables B.6 and B.7.

the number of infected employees compared to the other strategies. An interesting finding is that the number of infected employees in the scheduling plan increases as the average degree of the network increases but only for the strategies, Full allocation, and Partial allocation. In contrast, for the days-off strategy, such assertion is not always applicable; it would depend on the threshold value and capacity availability since the model aims to balance these criteria in the allocation process. For instance, for the networks, N1 and N3 the Partial allocation strategy results in an average number of infected employees of 36.27% and 47.80% respectively. On the contrary, the days-off strategy yields N1 = 10.65% and N3 = 10.24% of infected employees. Thus, the resulting value of infected employees for N3 is higher even though the network structure has a higher number of connections among employees. The results mentioned above can be better explained with the solutions in the right panel about the employee allocation plan, for which performance metrics are summarized in Table 2.

Second, for answering the question, *When to assign* the employees, the scheduling plan smooths the allocation based on the infection curve progression in the planning horizon. Thus, the lowest number of employees are allocated at the beginning of the week, increasing towards the end to flatten the infection curve, for all network structures. This allocation strategy reduces the number of infected employees in the planning period by 20%-45% compared to the Full allocation and Partial allocation strategies. Note that for the other strategies, such allocation pattern would differ as the threshold of infected employees allowed is higher and the capacity availability constraint is relaxed. Third, the employee category Medium risk (i.e., s_2) has the highest allocation rate compared to the other categories, followed in most cases by s_3 (High risk) and s_1 (Low risk). We can assert that these results are mostly dependent on the distribution of workload demand defined in the base case study in which s_2 corresponds to 45% of the total workload demand with a medium risk of infection, β. Since the model aims to maximize occupancy at the lower risk, it prioritizes the employee category with the least impact on infection progression. We also observe that the employee category s_3 is mostly allocated at the end of the time horizon, which is expected since the aim is to accomplish (to a certain extent) the lowest number of infections (according to the threshold value definition, α). We explore other configurations of the workload demand in the sensitivity analysis Section 5.

Regarding the questions *Whom to allocate* and for *How many days*, we observe that the model seeks to balance assigning a high number of employees with a short duration and a low number of employees with a high duration. Although the employee category s_2 has the highest workload demand allocated (%DC) for all network structures, it also has the highest number of allocation days discounted from the defined budget (%DA). For instance, in the contact network N2 the number of discounted days is $s_2 = 13.33\%$ compared with a 3.33% for both s_1 and s_3, which results in an average allocated days of $AL = 2.32$ per employee. In addition, we would expect that the average weekly demand coverage ($\overline{DC}$) and occupancy level ($\%OCC$) decrease as the number of interactions in the workplace increases. However, as shown in Table 2, while N1 results in the highest demand coverage, $\overline{DC} = 85\%$, N2 yields $\overline{DC} = 70\%$ and N3, $\overline{DC} = 72\%$. Thus, for a high number of interactions, as in N3, the demand coverage is higher than N2, but at the expense of a higher number of infections, $RI = 10.24$, versus $RI = 9.45$ in N2.

According to the findings, we deduce that a low average degree distribution of the network (i.e., low number of

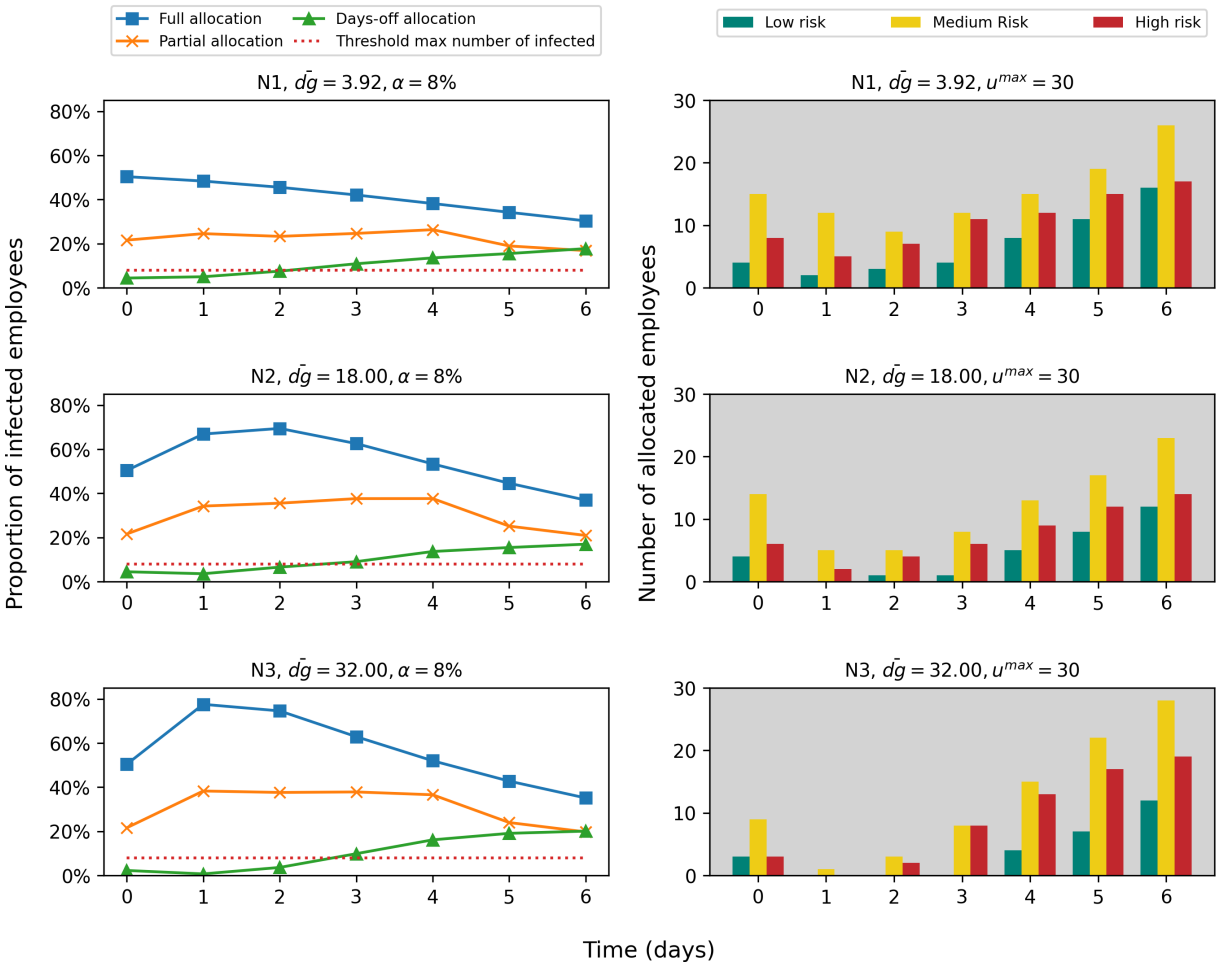

Figure 2: Disease progression (left panel) and optimal schedule (right panel) for different network structures and allocation strategies.

Contact network	Average infected *%RI*	Weekly demand coverage *%DC*			Budget discount allocation days *%DA*			Average allocated days, *AL*	Occupancy level *%OCC*	Total benefit κ
		s_1	s_2	s_3	s_1	s_2	s_3			
N1	10.65	80.00	93.33	83.33	-	-	-	2.66	56.20	366.97
N2	9.45	64.00	82.22	66.67	3.33	13.33	3.33	2.32	41.12	320.77
N3	10.24	60.00	82.22	73.33	3.33	10.00	-	2.35	42.33	321.67

Table 2: Performance indicators of the days-off scheduling model for different contact networks.

interactions) does not necessarily guarantee a low number of infections in the scheduling plan. Since the days-off scheduling model aims for a flexible scheme of allocation, that maximizes occupancy at the lower risk of infection, for a network with a low average degree distribution (e.g., $N1$), an increment in the number of infected employees (i.e., above the defined threshold value) results in the highest occupancy level at the highest benefit (lowest cost), N1: $\kappa = 366.97$. On the contrary, for a network with a high number of interactions, such as $N3$, the average number

of infected employees is lower, but with fewer average allocated days ($AL = 2.35$) and a lower occupancy level ($OCC = 42.33\%$). Thus, finding the optimal schedule configuration during a pandemic requires not only controlling the number of interactions among employees (e.g., safety measures, social distancing) but also defining the scheduling plan goals over the expected number of infected employees, allocation days, and capacity availability, so that the maximum occupancy can be balanced for the lower number of infected employees. In addition, the definition of a testing strategy plays an essential role in balancing the allocation[4]). We explore the impact on allocation decisions of α and τ in the Sensitivity analysis Section 5.

Overall, by implementing the days-off allocation strategy, we can flatten the infection curve while guaranteeing the minimum risk of infection (to a certain extent), the highest workplace occupancy, and weekly demand coverage. Of course, a decision-maker must define the ultimate goal of the plan and set a number of parameters (i.e., capacity availability, the threshold on the number of infected, and testing rate) accordingly to balance the employee allocation in the planning horizon.

5. Sensitivity analysis days-off scheduling model

In this section, we perform a sensitivity analysis on the solution obtained from the base case study. We aim to study how the days-off allocation approach performs under various scenarios. In Subsection 5.1 we analyze different testing strategies and the impact of the number of infected employees and threshold parameters on the allocation decisions and risk of infection. In Subsection 5.2 we further investigate the effects that particular workload demand configurations can have on the scheduling decisions. Finally, in Subsection 5.3, we analyze the computational performance of the proposed model and its capability to solve large instances.

5.1. Testing rate strategy and threshold on the number of infected employees

The base case study presented in Subsection 4.2 considered the same value of the testing rate, τ for all the employee categories, as well as a fixed parameter of the number of infected employees threshold, α. In this subsection, we perform a sensitivity analysis to the base case study to observe how changes in the testing rate and threshold parameters affect the scheduling decisions and infection rate in the time horizon. For the experiments we change the values of the parameters, α and τ one at a time by considering the Days-off allocation strategy and the contact network N2 ($\overline{dg} = 18.00$). The other parameters are the same as those defined in Subsection 4.1.

5.1.1. Testing strategy

The testing strategy defined in the workplace has a significant impact on the progression of the virus through the employee contact network. By increasing the testing rate (τ), the expected number of infected employees (RI) would decrease, allowing the workload demand to be increased without putting the employees at risk. We explore several

[4]Recall that for the base case we consider the same testing rate for the employee's categories.

testing strategies to assess the impact on the weekly demand coverage, $\%DC$, and the risk of infection on employee allocation. We define three testing strategies; same rate SR, incremental rate IR, and high risk rate HR. The SR strategy is as defined in the base case study, with an equal testing rate for all employee categories. The IR strategy considers an incremental testing policy, in which the employees are tested based on their risk of infection. Therefore, employees in category s_1 are tested at a lower rate than employees in category s_3. The testing strategy HR tests only the employees in the high risk category; it assumes that employees in the remaining categories observe the required workplace safety measures. We also evaluate the scenario without testing for all the employees.

For the experiments we define a base scenario of the testing strategies in which we set the testing rate as SR = 20% for all employee categories; IR = 15%, 20%, 33% for the $s1$, s_2, and s_3 categories, respectively; and HR = 1 for the s_3 category and zero for $s1$ and s_2. To investigate the effect of testing across the three testing strategies, we scale the base scenario rate values above and below in 2% steps. In addition, to evaluate the effect of the threshold parameter on the solutions, we consider three scenarios of $\alpha = 4, 8, 16$. Figure 3 shows the expected number of infected employees for different testing strategies and α scenarios[5]. The x-axis refers to the testing rate, with 1 being the previously defined base scenario values. Thus, a testing rate of 0 implies no testing, while numbers greater than one indicate an increase in the testing rate from the reference values. The results follow a similar pattern for all the three scenarios of α. For low testing rates $\approx$ [0 - 6%], there is a minimum deviation from the threshold parameter (stays within the allowed range), α. As the testing rate increases, a higher number of employees are allocated, and therefore the RI reaches a peak but starts decreasing for higher testing rates, $\tau \geq 20\%$.

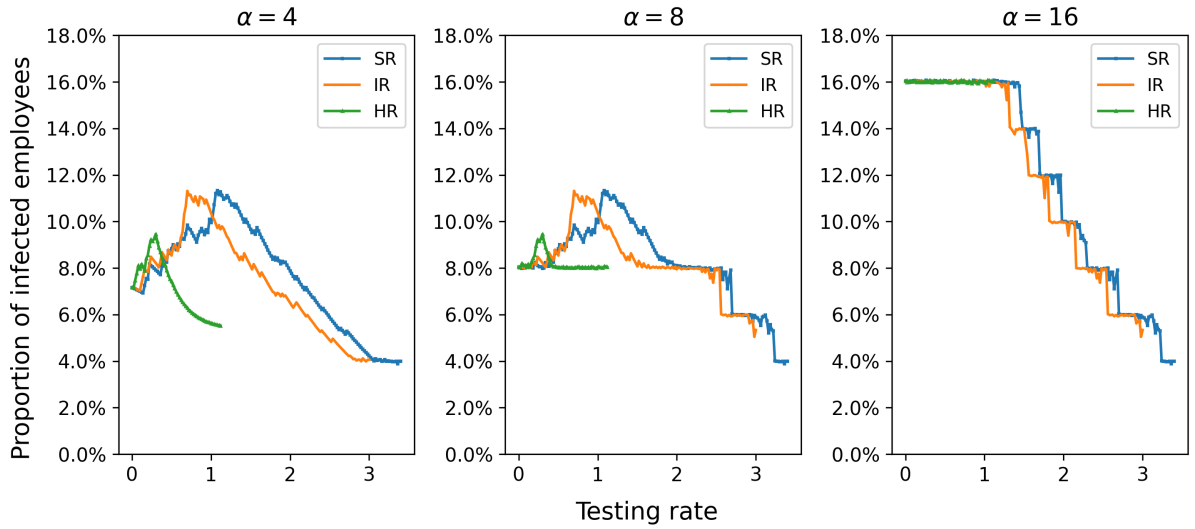

Figure 3: Comparison of proportion of infected employees for variations in testing strategy and threshold value. Testing strategies, Same Rate, SR; Incremental rate, IR; High rate, HR. The x-axis refers to as τ where 1 indicates the base scenario testing rates.

We also observe a phase shift pattern that varies among the testing strategies. For instance, in the second figure,

[5]Extended numerical results can be found in Appendix C, Tables C.9–C.11.

with an $\alpha = 8$, the SR strategy yields the lowest RI at testing rates ranging from [0 - 20%], while for the IR strategy, the lowest number of infected employees lies on testing rates higher than 20%. Like the other testing strategies, HR provides the highest RI for low testing rates, decreasing as the testing increases. For a high constrained scenario, i.e., $\alpha = 4$, RI decreases as increasing the testing rate, whereas it remains constant for $\alpha = 8, 16$. It is worth noting that the lowest RI for the HR strategy is around the threshold value. In contrast, for SR and IR, with $\alpha = 8, 16$, the expected number of infected employees falls below the threshold parameter as the testing rate increases. These results may be explained by the fact that the HR strategy focuses on testing only the high risk employees disregarding the other categories that may be in contact with high risk employees in the contact network.

Another relevant aspect to analyze is how the testing strategy influences the allocation decisions for the different employee categories. Figure 4 shows the allocation distribution for the base scenario testing rates, considering $\alpha = 8$[6]. As stated in Subsection 4.2, the scheduling plan smooths the allocation based on the progression of infection curves. By comparing the testing strategies, we notice that the employee allocation distribution varies among the strategies. While the SR strategy prioritizes the allocation of the s_2 category, the IR distributes the employees, prioritizing those with the higher testing rate at the end of the time horizon. For the HR strategy, which focuses on testing only the s_3 category, the employee types s_1 and s_2 are allocated at the beginning of the time horizon, and the s_3 at the end, which indicates that the model is flattening the infection curve, due to the low rate of testing of the other employee categories. When testing is not performed, the employees are allocated at the beginning of the time horizon, leaving no allocation for periods 4 – 6. Thus, under this strategy, the organization would be required to go on full remote work at the end of the time horizon to limit the spread of the virus to the defined threshold value, α.

Table 3 summarizes the performance indicators for the base scenario testing strategies, with $\alpha = 8$ and $u^{\max} = 30$. The HR strategy gives the highest benefit of the scheduling plan for the base scenario testing rates. Thus, by testing (every day) all of the employees in the s_3 category, the testing strategy results in 8.05% of employees infected at the end of the time horizon, for a $\overline{DC}$ of 76% and AL of 2.42 days. A higher weekly demand coverage of 81% and AL of 2.51 is obtained with the IR strategy, but with a higher number of infected employees, $RI = 10.37\%$. However, if the testing rate is increased by 15% (See Table C.10 in Appendix C) for all of the employee categories, the RI will result in 5.9% with a 100% weekly demand coverage, and $AL = 2.9$ days, obtaining, therefore, a total benefit of $\kappa = 441$. As expected, the no testing strategy yields the lowest benefit with an $RI = 8.05\%$ and $\overline{DC} = 56\%$. By implementing this strategy, the decision-maker can opt for the lowest occupancy without exceeding the defined threshold of the number of infected employees, $\alpha = 8$. However, the average number of allocated days, AL, is the lowest, indicating that the employees will be present in the workplace on average, 1.69 days. In addition, as shown in Figure 4 this strategy concentrates the allocation at the beginning of the time horizon, requiring home working at the end of the period, which might not be realistic for some organizations.

Overall, we find that the IR strategy outperforms the SR and HR strategies. The expected number of infected

[6]Extended numerical results can be found in Appendix C, Table C.8.

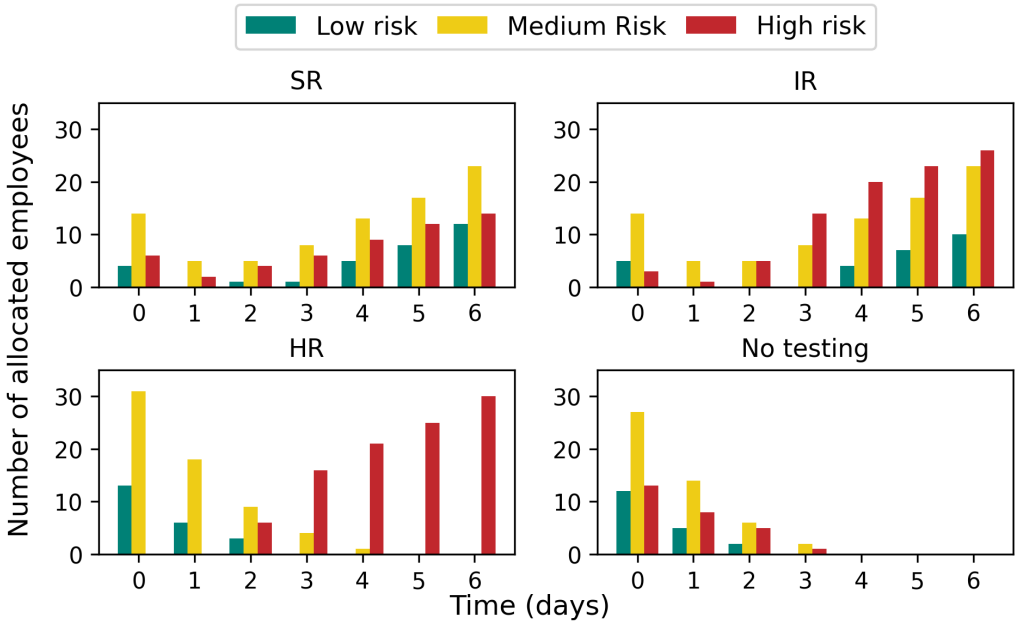

Figure 4: Employee allocation for the testing strategies: Same Rate, SR; Incremental rate, IR; High rate, HR; network: N2; $\alpha = 8$.

Testing strategy	Testing rate (%)			Average infected	Average weekly demand coverage,	Budget discount allocation days	Occupancy level	Average allocated days, AL	Total benefit
	s_1	s_2	s_3	$\%RI$	$\%\overline{DC}$	$\%\overline{DA}$	$\%OCC$		κ
SR	20	20	20	9.94	73.00	20.00	40.00	2.31	320.77
IR	15	15	33	10.37	81.00	20.00	48.00	2.51	342.85
HR	0	0	100	8.05	76.00	20.00	44.00	2.42	348.35
No testing	-	-	-	8.05	56.00	36.66	24.00	1.69	255.33

Table 3: Summary of performance indicators for evaluating different testing strategies.

employees can be reduced by distributing the tests among all employee categories based on their risk, without needing to test everyone every day. This strategy also ensures a smooth allocation of the employees in the time horizon by flattening the infection curve. Moreover, increasing the threshold value increases the expected number of infected employees, but the impact can be mitigated by increasing the testing rate. The phase shift pattern that we described results from the days-off scheduling model balancing the allocation among the employee categories to guarantee the maximum benefit at a lower risk of infection. In the next subsection, we explore how varying the threshold parameter can affect the allocation decisions in the scheduling plan.

5.1.2. Threshold on allocation decisions and risk of infection

Implementing a scheduling plan during outbreaks requires the definition of the threshold for the number of infected employees, which the decision-makers sets. The definition of α may be controversial because despite establishing safety measures, allowing many employees present in the workplace would inevitably lead to a certain number of

infections. As we showed in the previous section, increasing α will also increase the number of infected employees due to the flexibility of the days-off scheduling model. However, the risk of infection can be reduced (to a certain extent) by increasing the testing rate. We remark that since the model aims to maximize workplace occupancy, α leads to an upper bound in the allocation process. We have defined a large enough value of the penalty cost c^{IF}, such that the slack variable Γ, stay at zero, if possible (refer to Constraint (7)).

We explore how the allocation decisions and risk of infection are affected by changes in the threshold parameter. For the experiments, we consider the base scenario testing rates, varying the values by ±15% for the different testing strategies[7]. Figure 5 summarizes the results. The left panel compares the average proportion of infected employees for different values of α, and the right panel shows the related weekly demand coverage[8]. The results are consistent with the analyses performed in Subsection 5.1.1. We observe that for all configurations, when α increases, so does $\overline{DC}$. For low testing rates (Figs. (a)–(b)), variations in α do not significantly affect the $\overline{DC}$ and RI performance indicators among the testing strategies; the variations are more evident as the testing rate increases.

For the base scenario (Figs.(c)–(d)) the testing strategy IR outperforms SR and HR strategies in weekly demand coverage, $\overline{DC}$, for variations in α. For the RI the differences are minimal, with the exception of the HR strategy, which results in a low number of infected employees for low $alpha$ values [0 -10]. We also notice that regardless of the defined α value, increasing the testing rate increases the weekly demand coverage for lower values of RI. For instance, for the base scenario (Figs.(c)–(d)) with $\alpha = 10$, the IR strategy yields $\overline{DC} = 81\%$ and $RI = 10.4\%$. However, by increasing the testing rate by 15% (Figs.(e)–(f)), $\overline{DC} = 100\%$ with $RI = 10\%$, which results in a higher benefit of the scheduling plan.

The results reveal that the setting of α must be combined with the appropriate testing approach based on the level of interactions in the workplace. Risk averse decision makers who desire to keep the number of infected personnel to a minimum (e.g., $alpha = 0$) while maintaining the maximum occupancy levels can achieve this goal by using the testing strategies IR and SR. However, high testing rates will be required to attain such an objective.

5.2. Workload demand configuration

To understand the effect of different configurations of the workload demand on the optimal solution, we define three different settings of r_{is}, as described in Table 4. The first setting is as we defined in the base case study, where medium risk employees, s_2, have the highest value. For the second case, we assume that there is an equal number of employees in each category, and for the third configuration, we consider that high risk employees, s_3, have the highest value. For the experiments, we employ the contact network N2 and the same input parameters as defined in Section 4.2.

Table 4 summarizes the performance indicators for the different workload demand configurations. The setting 2 results in the highest benefit of the scheduling plan, $\kappa = 325.78$, with an average number of allocated employees of

[7]Note that for the testing strategy HR, the testing rate can only be increased up to 100%, considering the sensitivity of the test σ.

[8]Extended numerical results for each scenario can be found in Appendix C, Tables C.12 and C.13.

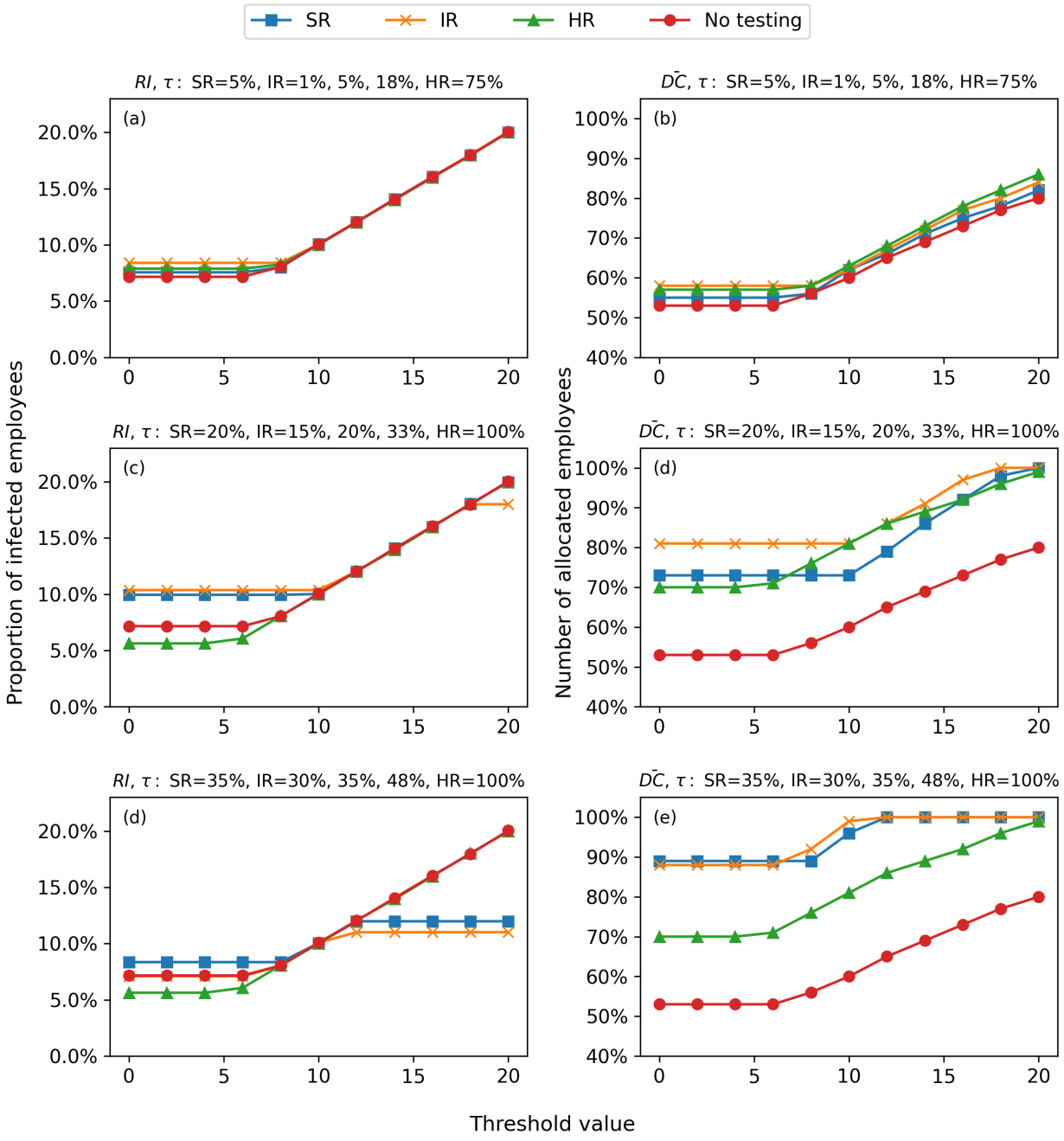

Figure 5: Expected proportion of infected employees (left panel) and weekly demand coverage (right panel) for several α values and testing strategies.

$\overline{DC}$ = 73.84% and RI = 9.94%. The setting 1 has similar results, $\overline{DC}$ = 70.96% and RI = 9.95%, although the weekly distribution of employees varies, resulting in a lower benefit of the scheduling plan, κ = 320.77, because it is discounting more days from the budget discount. As expected the setting 3, which considers a high number of

employees in the high risk category, results in the lower benefit of the scheduling plan, $\kappa = 319.88$ and the highest number of employees infected, $RI = 10.29\%$ with a $\overline{DC} = 73.55\%$.

Setting	Number of employees r_{is}			Weekly demand coverage $\%\overline{DC}$			Average infected $\%RI$	Budget discount allocation days $\%\overline{DA}$	Occupancy level $\%OCC$	Average allocated days AL	Total benefit κ
	s_1	s_2	s_3	s_1	s_2	s_3					
1	25	45	30	64.00	82.22	66.66	9.95	20	41.11	2.32	320.77
2	34	33	33	61.76	90.09	69.69	9.94	10	41.84	2.32	325.78
3	30	25	45	63.33	84.00	73.33	10.29	10	42.82	2.41	319.88

Table 4: Performance indicator for different workload demand configurations.

Although the differences among the settings look minimal in terms of the $\%RI$ and $\overline{DC}$, the most substantial difference is found in the distribution of allocated employees as shown in Figure 6. We observe that according to the setting, employees in each category are allocated differently [9] so that to balance the risk of infection and the occupancy levels accordingly. We remark that even a small percentage reduction in the number of infected employees is a significant gain during a pandemic. Therefore, we can state that introducing preventive measures to decrease the number of employees in the high risk groups can help stem the number of infections in the workplace while guaranteeing a high occupancy level.

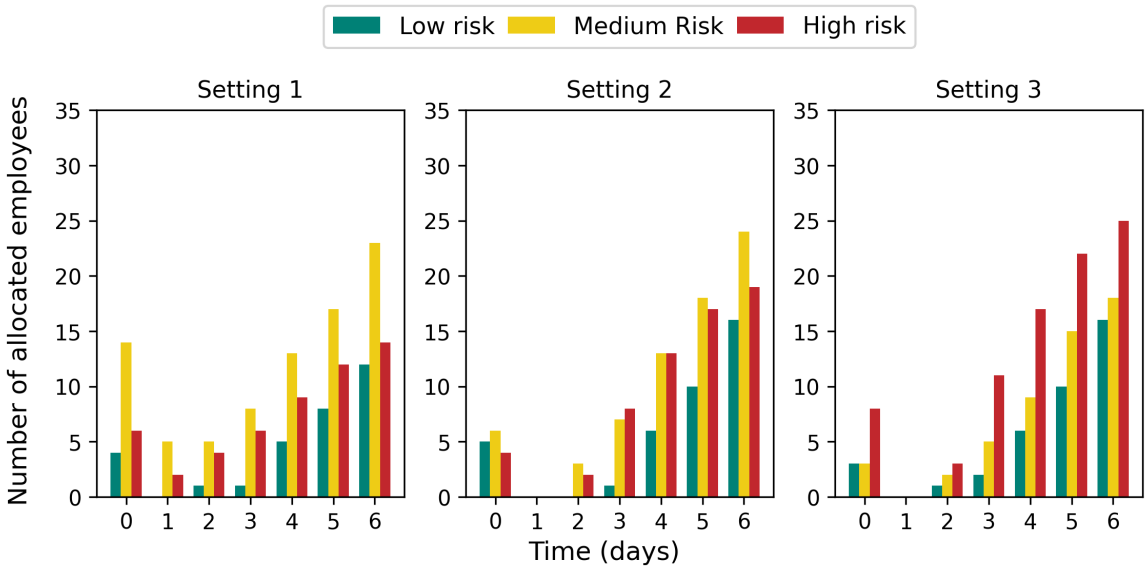

Figure 6: Employee allocation for different workload demand configurations. setting 1: $s_1 = 25$ $s_2 = 45$ $s_3 = 30$; setting 2: $s_1 = 34$ $s_2 = 33$ $s_3 = 33$; setting 3: $s_1 = 30$ $s_2 = 25$ $s_3 = 45$.

[9] Extended numerical results can be found in Appendix C, Table C.14.

5.3. Computational performance days-off scheduling model

The days-off scheduling model that we propose has a complex combinatorial structure. Due to the underlying contact network used to compute the disease progression, the number of constraints and variables may increase according to the network structure and number of nodes. We performed a sensitivity analysis to assess the computational performance of the days-off scheduling model and its capability to solve large instances. Table 5 shows the performance in terms of solution gap (%) and CPU time (s) of 12 instances. We consider a scale-free network varying the number of nodes, n, and network measures for each instance. We consider the input parameters, $\alpha = 8$; $u^{\max} = 30$; testing strategy, IR. Each group of instances corresponds to a network with n = 100, 300, 600, and 1000, differing by degree distribution, $\overline{dg}$, clustering coefficient, $\overline{C}$, and average path length, $\bar{k}$.

	Instance characteristics				Computational time / Size			
Instance	Number of nodes n	Average degree $\overline{dg}$	Clustering coefficient $\overline{C}$	Path length $\bar{k}$	Variables (thousands)	Constraints (thousands)	CPU time (s)	Gap (%)
1	100	3.92	0.18	2.86	3.00	1.00	0.17	0.00
2	100	18.00	0.28	1.86	3.00	1.00	0.13	0.00
3	100	32.00	0.41	1.68	3.00	1.00	0.13	0.00
4	300	3.97	0.08	3.58	9.30	3.00	0.30	0.00
5	300	19.33	0.14	2.18	9.30	3.00	0.34	0.00
6	300	37.33	0.21	1.90	9.30	3.00	0.33	0.00
7	600	3.99	0.05	3.89	18.60	6.00	1.52	0.00
8	600	19.67	0.08	2.41	18.60	6.00	10.08	0.00
9	600	38.67	0.13	2.04	18.60	6.00	0.72	0.00
10	1000	3.99	0.04	3.94	31.10	10.00	2.14	0.20
11	1000	19.80	0.06	2.55	31.10	10.00	5.64	0.20
12	1000	39.20	0.09	2.17	31.10	10.00	1.42	0.20

Table 5: Comparative of performance evaluation days-off scheduling model.

We evaluate several standard methods to improve the solution performance of the model. We define *presolve=1* to eliminate redundant variables and constraints, which reduced the size of the model to approximately 70% of its original size, considerably improving the computational time. For instances 1–9, we set the solution gap to 0%, which guarantees an optimal integer solution in a few seconds, independently of the size of the network. For instances 10–12, related to networks with 1000 nodes, we set the solution gap to 0.2%, since for lower values than this gap, the model was unable to find an optimal solution after 30 minutes of running time. Still, the solutions satisfy integrality while guaranteeing optimality. The results show that the proposed days-off scheduling model can solve large instances of realistic size within a short computational time. Although the computational effort increases with the size of the network, the quality of the solution remains within acceptable limits.

6. Concluding remarks

Personnel scheduling is a complex and time-consuming process that significantly impacts organizational operations. The complexity of the PSP increases during unexpected disruptive events that put the staff and the organization's goals at risk, requiring efficient staffing policies. In response to the recent COVID-19 pandemic, we proposed a novel MILP model to solve a days-off scheduling model coupled with an MMCA modeling framework that computes the probability of infection transmission of the staff that works in close contact. The model aims to maximize workplace occupancy while minimizing the number of infected employees in the time horizon. Our findings highlight the importance of efficient staffing and scheduling practices for organizations that must maintain their operations during disease outbreaks.

We studied the impact of disease spread on staffing and scheduling decisions considering a network-based epidemiological approach. The proposed days-off scheduling model determined when and which employee to allocate as well as the allocation length while ensuring the minimum number of infected employees in the time horizon. We studied the effect of the contact network structure on employee allocation by comparing three strategies: *Full allocation*, *Partial allocation*, and *Days-off allocation*. We showed that the days-off strategy outperforms the cases when the employees are fully and partially allocated; this strategy decreased the expected number of infected employees by 20%-45% compared to the other strategies. By defining a threshold value over the expected number of infected employees and capacity availability constraints, the Days-off allocation strategy can accomplish weekly demand coverage and occupancy levels while guaranteeing safety in the workplace (to a certain extent). The findings revealed that in the context of personnel scheduling, a low average degree distribution of the network, does not necessarily guarantee lower infection rates. This finding is noteworthy since the most standard practice in organizations during disease outbreaks has been to impose social distancing rules in the workplace (D'angelo et al., 2021). Aside from the employee interactions, other factors have to be considered, such as the definition of the threshold value of the expected number of infected employees and the testing strategy which has a direct impact on allocation decisions. As a result, a tailored staffing and scheduling plan would have to be developed in accordance with management's priorities and needs.

We performed a sensitivity analysis to explore the impact of different testing strategies and variations of the expected number of infected employees on the allocation decisions and risk of infection. We evaluated three testing strategies: *Same rate*, *Incremental rate*, and *High rate*. We found that the *Incremental testing rate*, which tests the employees according to their risk of infection, outperformed the other strategies in both weekly demand coverage and the average number of infected employees. However, the selection of the testing strategy must be carefully defined according to the threshold value of the expected number of infected employees. Risk-averse decision-makers who prefer to keep a low value of infected employees while increasing occupancy would have to increase testing rates to reach this goal; nonetheless, even with low occupancy levels, a certain proportion of infected employees is unavoidable. We showed that the most efficient balance between the risk of infection and workplace occupancy is

obtained with the *Same rate* and *Incremental rate* testing strategies. In addition, we assessed the impact of workload demand configuration on allocation decisions. The results showed that introducing pharmaceutical and not pharmaceutical interventions in the workplace (e.g., vaccination, use of masks) to reduce the number of employees in the high risk groups would contribute to decreasing the number of infections in the workplace with high occupancy levels and low testing rates.

The proposed days-off scheduling model during disease outbreaks can be implemented and used in real organizational settings to guide staff planning. The model can solve large instances with low computational effort while guaranteeing optimality. Of course, for real-world applications, additional factors, such as data collection, to capture the number of interactions among employees, the individual probability of transmission, and priority levels, would need to be considered. The underlying contact network of employees is the most crucial data to collect; yet, this type of data collection has previously been handled (Génois et al., 2015) by giving wearable sensors to people for recording face-to-face contacts in an office building. For practical applications of the proposed approach, we remark that the scheduling policies during disease outbreaks should be carefully examined, as such decisions impact people's lives and well-being.

The model can be extended to incorporate additional features tailored to specific sectors. For instance, in the service sector (i.e., retail, call center, health, postal services) is relevant to consider employee preferences of allocation and labor flexibility by introducing multiskilled staff. In addition, it would be interesting to consider a bipartite weighted network to represent the interactions of the employees with external visitors and assess the trade-off between demand coverage, supply, and risk of infection. Further extensions to the model can include uncertainty in disease transmission probability and allocation days to capture the system's natural variability and provide robust scheduling decisions in a high-risk context. The aspects above can be easily included in the current model without modifying the main structure. Finally, the modeling framework we propose considering a network-based epidemiological approach can be broadly applied to any outbreak disease with similar characteristics to the SARS-CoV-2 virus, accounting for virus transmission via droplet and airborne routes.

Acknowledgements

This work was partially funded by the Center of Advanced Systems Understanding (CASUS), which is financed by Germany's Federal Ministry of Education and Research (BMBF) and by the Saxon Ministry for Science, Culture, and Tourism (SMWK) with tax funds on the basis of the budget approved by the Saxon State Parliament.

References

Abdin, A. F., Fang, Y.-P., Caunhye, A., Alem, D., Barros, A., & Zio, E. (2021). An optimization model for planning testing and control strategies to limit the spread of a pandemic–the case of COVID-19. *European journal of operational research*, .

Albert, R., & Barabási, A.-L. (2002). Statistical mechanics of complex networks. *Reviews of modern physics*, *74*, 47.

Arenas, A., Cota, W., Gómez-Gardeñes, J., Gómez, S., Granell, C., Matamalas, J. T., Soriano-Paños, D., & Steinegger, B. (2020). Modeling the spatiotemporal epidemic spreading of COVID-19 and the impact of mobility and social distancing interventions. *Physical Review X*, *10*, 041055.

Aslan, S., & Türkakın, O. H. (2021). A construction project scheduling methodology considering COVID-19 pandemic measures. *Journal of Safety Research*, .

Bagger, N.-C. F., van der Hurk, E., Hoogervorst, R., & Pisinger, D. (2022). Reducing disease spread through optimization: Limiting mixture of the population is more important than limiting group sizes. *Computers & Operations Research*, (p. 105718).

Baker, K. R. (1976). Workforce allocation in cyclical scheduling problems: A survey. *Journal of the Operational Research Society*, *27*, 155–167.

Barabási, A.-L., & Albert, R. (1999). Emergence of scaling in random networks. *science*, *286*, 509–512.

Batista, A., Pozo, D., & Vera, J. (2020). Stochastic time-of-use-type constraints for uninterruptible services. *IEEE Transactions on Smart Grid*, *11*, 229–232.

Van den Bergh, J., Beliën, J., De Bruecker, P., Demeulemeester, E., & De Boeck, L. (2013). Personnel scheduling: A literature review. *European journal of operational research*, *226*, 367–385.

Block, P., Hoffman, M., Raabe, I. J., Dowd, J. B., Rahal, C., Kashyap, R., & Mills, M. C. (2020). Social network-based distancing strategies to flatten the COVID-19 curve in a post-lockdown world. *Nature Human Behaviour*, *4*, 588–596.

Boccaletti, S., Latora, V., Moreno, Y., Chavez, M., & Hwang, D.-U. (2006). Complex networks: Structure and dynamics. *Physics reports*, *424*, 175–308.

Bollobás, B. (2012). *Graph theory: an introductory course* volume 63. Springer Science & Business Media.

Brucker, P., Qu, R., & Burke, E. (2011). Personnel scheduling: Models and complexity. *European Journal of Operational Research*, *210*, 467–473.

Choi, T.-M. (2021). Fighting against COVID-19: what operations research can help and the sense-and-respond framework. *Annals of Operations Research*, (pp. 1–17).

Cohon, J. L. (2004). *Multiobjective programming and planning* volume 140. Courier Corporation.

CubasAtienzar, A., Bell, F., Byrne, R., Buist, K., Clark, D. J., Cocozza, M., Collins, A., Cuevas, L., Duvoix, A., Easom, N. et al. (2021). Accuracy of the mologic covid-19 rapid antigen test: a prospective multi-centre analytical and clinical evaluation. *Wellcome Open Research*, *6*, 132.

D'angelo, D., Sinopoli, A., Napoletano, A., Gianola, S., Castellini, G., Del Monaco, A., Fauci, A. J., Latina, R., Iacorossi, L., Salomone, K. et al. (2021). Strategies to exiting the covid-19 lockdown for workplace and school: A scoping review. *Safety science*, *134*, 105067.

Davoodi, M., Senapati, A., Mertel, A., Schlechte-Welnicz, W., & Calabrese, J. M. (2022). Optimal workplace occupancy strategies during the COVID-19 pandemic. *arXiv preprint arXiv:2204.01444*, .

Ely, J., Galeotti, A., & Steiner, J. (2021). Rotation as contagion mitigation. *Management Science*, *67*, 3117–3126.

Ernst, A. T., Jiang, H., Krishnamoorthy, M., Owens, B., & Sier, D. (2004a). An annotated bibliography of personnel scheduling and rostering. *Annals of Operations Research*, *127*, 21–144.

Ernst, A. T., Jiang, H., Krishnamoorthy, M., & Sier, D. (2004b). Staff scheduling and rostering: A review of applications, methods and models. *European journal of operational research*, *153*, 3–27.

Génois, M., Vestergaard, C. L., Fournet, J., Panisson, A., Bonmarin, I., & Barrat, A. (2015). Data on face-to-face contacts in an office building suggest a low-cost vaccination strategy based on community linkers. *Network Science*, *3*, 326–347.

Gómez, S., Arenas, A., Borge-Holthoefer, J., Meloni, S., & Moreno, Y. (2010). Discrete-time markov chain approach to contact-based disease spreading in complex networks. *EPL (Europhysics Letters)*, *89*, 38009.

Gómez-Gardeñes, J., de Barros, A. S., Pinho, S. T., & Andrade, R. F. (2015). Abrupt transitions from reinfections in social contagions. *EPL (Europhysics Letters)*, *110*, 58006.

Granell, C., Gómez, S., & Arenas, A. (2013). Dynamical interplay between awareness and epidemic spreading in multiplex networks. *Physical review letters*, *111*, 128701.

Granell, C., Gómez, S., & Arenas, A. (2014). Competing spreading processes on multiplex networks: awareness and epidemics. *Physical review E*, *90*, 012808.

Guerriero, F., & Guido, R. (2021). Modeling a flexible staff scheduling problem in the era of COVID-19. *Optimization Letters*, (pp. 1–21).

Güler, M. G., & Geçici, E. (2020). A decision support system for scheduling the shifts of physicians during COVID-19 pandemic. *Computers & Industrial Engineering*, *150*, 106874.

Harapan, H., Itoh, N., Yufika, A., Winardi, W., Keam, S., Te, H., Megawati, D., Hayati, Z., Wagner, A. L., & Mudatsir, M. (2020). Coronavirus disease 2019 (COVID-19): A literature review. *Journal of infection and public health*, *13*, 667–673.

Hazarie, S., Soriano-Paños, D., Arenas, A., Gómez-Gardeñes, J., & Ghoshal, G. (2021). Interplay between population density and mobility in determining the spread of epidemics in cities. *Communications Physics*, *4*, 1–10.

Jordan, E., Shin, D. E., Leekha, S., & Azarm, S. (2021). Optimization in the context of COVID-19 prediction and control: A literature review. *IEEE Access*, .

Karin, O., Bar-On, Y., Milo, T., Katzir, I., Mayo, A., Korem, Y., Dudovich, B., Yashiv, E., Zehavi, A., Davidovich, N. et al. (). Adaptive cyclic exit strategies from lockdown to suppress covid-19 and allow economic activity. medrxiv (2020). *Available at doi. org/10.1101/2020.04*, *4*.

Keeling, M., & Eames, K. (2005a). Jr soc. *Interface*, *2*, 295–307.

Keeling, M. J., & Eames, K. T. (2005b). Networks and epidemic models. *Journal of the royal society interface*, *2*, 295–307.

Kiss, I. Z., Miller, J. C., Simon, P. L. et al. (2017). Mathematics of epidemics on networks. *Cham: Springer*, *598*.

Larremore, D. B., Shew, W. L., & Restrepo, J. G. (2011). Predicting criticality and dynamic range in complex networks: effects of topology. *Physical review letters*, *106*, 058101.

Lelieveld, J., Helleis, F., Borrmann, S., Cheng, Y., Drewnick, F., Haug, G., Klimach, T., Sciare, J., Su, H., & Pöschl, U. (2020). Model calculations of aerosol transmission and infection risk of COVID-19 in indoor environments. *International Journal of Environmental Research and Public Health*, *17*, 8114.

Li, H., Liu, S.-M., Yu, X.-H., Tang, S.-L., & Tang, C.-K. (2020). Coronavirus disease 2019 (COVID-19): current status and future perspectives. *International journal of antimicrobial agents*, *55*, 105951.

Lim, C. Y., Bohn, M. K., Lippi, G., Ferrari, M., Loh, T. P., Yuen, K.-Y., Adeli, K., Horvath, A. R. et al. (2020). Staff rostering, split team arrangement, social distancing (physical distancing) and use of personal protective equipment to minimize risk of workplace transmission during the covid-19 pandemic: a simulation study. *Clinical biochemistry*, *86*, 15–22.

Lyngse, F. P., Mortensen, L. H., Denwood, M. J., Christiansen, L. E., Moller, C. H., Skov, R. L., Spiess, K., Fomsgaard, A., Lassauniere, R., Rasmussen, M. et al. (2021). SARS-CoV-2 Omicron VOC transmission in Danish households. *medRxiv*, .

Matamalas, J. T., Gómez, S., & Arenas, A. (2020). Abrupt phase transition of epidemic spreading in simplicial complexes. *Physical Review Research*, *2*, 012049.

Mauras, S., Cohen-Addad, V., Duboc, G., Dupré la Tour, M., Frasca, P., Mathieu, C., Opatowski, L., & Viennot, L. (2021). Mitigating COVID-19 outbreaks in workplaces and schools by hybrid telecommuting. *PLoS computational biology*, *17*, e1009264.

Musliu, N., & Winter, F. (). Physician scheduling during a pandemic. *Integration of Constraint Programming, Artificial Intelligence, and Operations Research*, (p. 456).

Newman, M. (2018). *Networks*. Oxford university press.

Newman, M. E., Watts, D. J., & Strogatz, S. H. (2002). Random graph models of social networks. *Proceedings of the national academy of sciences*, *99*, 2566–2572.

Özder, E. H., Özcan, E., & Eren, T. (2020). A systematic literature review for personnel scheduling problems. *International Journal of Information Technology & Decision Making*, *19*, 1695–1735.

Qin, R., Nembhard, D. A., & Barnes II, W. L. (2015). Workforce flexibility in operations management. *Surveys in Operations Research and Management Science*, *20*, 19–33.

Rachaniotis, N. P., Dasaklis, T. K., & Pappis, C. P. (2012). A deterministic resource scheduling model in epidemic control: A case study. *European Journal of Operational Research*, *216*, 225–231.

Rawson, T., Brewer, T., Veltcheva, D., Huntingford, C., & Bonsall, M. B. (2020). How and when to end the COVID-19 lockdown: an optimization approach. *Frontiers in Public Health*, (p. 262).

754 Sánchez-Taltavull, D., Castelo-Szekely, V., Candinas, D., Roldán, E., & Beldi, G. (2021). Modelling strategies to organize healthcare workforce during pandemics: application to COVID-19. *Journal of theoretical biology*, *523*, 110718.

756 Sanchez-Taltavull, D., Castelo-Szekely, V., Murugan, S., Rollenske, T., Ganal-Vonarburg, S. C., Buchi, I., Keogh, A., Li, H., Salm, L., Spari, D. et al. (2021). Regular testing of asymptomatic healthcare workers identifies cost-efficient SARS-cov-2 preventive measures. *medRxiv*, .
758 doi:https://doi.org/10.1371/journal.pone.0258700.

Seccia, R. (2020). The nurse rostering problem in COVID-19 emergency scenario. *Tech-nical Report*, .

760 Shereen, M. A., Khan, S., Kazmi, A., Bashir, N., & Siddique, R. (2020). COVID-19 infection: Emergence, transmission, and characteristics of human coronaviruses. *Journal of advanced research*, *24*, 91–98.

762 Valdano, E., Ferreri, L., Poletto, C., & Colizza, V. (2015). Analytical computation of the epidemic threshold on temporal networks. *Physical Review X*, *5*, 021005.

764 Wang, W., Tang, M., Stanley, H. E., & Braunstein, L. A. (2017). Unification of theoretical approaches for epidemic spreading on complex networks. *Reports on Progress in Physics*, *80*, 036603.

766 Wang, Z., Guo, Q., Sun, S., & Xia, C. (2019). The impact of awareness diffusion on sir-like epidemics in multiplex networks. *Applied Mathematics and Computation*, *349*, 134–147.

768 Watts, D. J., & Strogatz, S. H. (1998). Collective dynamics of 'small-world'networks. *nature*, *393*, 440–442.

WHO COVID-19 (2020). Dashboard. Geneva: World Health Organization. Available from: https://covid19.who.int/.

770 World Health Organization and others (2022). Enhancing response to Omicron SARS-CoV-2 variant. Available from: www.who.int/publications/m/item/enhancing-readiness-for-omicron-(b.1.1.529)-technical-brief-and-priority-actions-for-memberstates (21
772 January 2022).

Zucchi, G., Iori, M., & Subramanian, A. (2021). Personnel scheduling during COVID-19 pandemic. *Optimization Letters*, *15*, 1385–1396.

Appendix A. Network properties description

The spreading of a virus through a contact network depends on several fundamental measures that can be obtained from the defined graph, G. In this study, we focus on the network measures: 1. node degree (heterogeneity in the number of contacts); 2. clustering of contacts, and the 3. average path length of the network, described as follows:

1. *Node degree (dg)*:

   The degree of node i corresponds to the number of connections it has. For the adjacency matrix $\mathbf{A}(=a_{ij})$ the degree of node i can be computed as,

$$dg_i = \sum_{j=1}^{E} a_{ij} \quad \forall i \in E \tag{A.1}$$

2. *Average clustering coefficient (C)*:

   The local clustering coefficient for node i is defined as the ratio of the number of edges in its neighbors and the total number of all edges possible with the neighbors (Watts & Strogatz, 1998; Newman, 2018). This network measure quantifies how the neighbors of node i are connected with each other. Let us denote the number of edges among the neighbors of node i by Q_i. Also if the node i has degree dg_i, then the total number of possible edges is $\frac{dg_i(dg_i-1)}{2}$. Therefore, the mathematical expression of the local clustering coefficient for node i can be written as:

$$C_i = \frac{2Q_i}{dg_i(dg_i - 1)},$$

   Finally, the average clustering coefficient ($\overline{C}$) can be obtained as:

$$\overline{C} = \frac{1}{n} \sum_{i \in G} C_i. \tag{A.2}$$

3. *Average path length ($\bar{k}$)*:

   The shortest path between node i and node j refers to the collection of minimum number edges through which node i and node j can be connected. Let $d(i, j)$ be the length (i.e, number of edges in shortest path) of the shortest path between nodes i and j. Then the average path length ($\bar{k}$) for a network consisting of number of nodes can be expressed as follows (Albert & Barabási, 2002):

$$\bar{k} = \sum_{i,j \in \mathcal{V}} \frac{d(i, j)}{n(n-1)} \tag{A.3}$$

Appendix B. Extended numerical results days-off scheduling model: base case

This section presents the extended numerical results of the days-off scheduling model for the base case problem detailed in Subsection 4.2. Table B.6 details the proportion of infected employees for the different allocation strategies: Full allocation, Partial allocation, Days-off allocation, and network structures: N1, N2, N2. Similarly, Table B.7 shows the proportion of allocated employees for the allocation strategies and network structures. We also present the results for the different employee categories: High risk, s_1, Medium risk, s_2, and Low risk, s_3. Note that for the Full allocation and Partial allocation strategies, we do not discriminate by type of network because the results are the same for each case.

Table B.6: Proportion of infected employees for different network structures and allocation strategies.

	N1			N2			N3		
t	Full allocation	Partial allocation	Days-off allocation	Full allocation	Partial allocation	Days-off allocation	Full allocation	Partial allocation	Days-off allocation
0	50.35	21.58	4.39	50.35	21.58	4.45	50.35	21.58	2.25
1	48.35	24.53	4.98	66.87	34.22	3.56	77.56	38.26	0.69
2	45.54	23.29	7.51	69.43	35.53	6.55	74.57	37.60	3.62
3	42.05	24.62	10.87	62.55	37.61	9.03	62.90	37.84	9.84
4	38.17	26.32	13.53	53.34	37.63	13.63	51.96	36.55	16.12
5	34.19	18.94	15.50	44.56	25.13	15.44	42.74	23.96	19.08
6	30.31	16.83	17.74	36.92	20.91	16.96	35.10	19.71	20.08

Table B.7: Proportion of allocated employees per different testing strategies and employee category.

	Full allocation *%DC*			Partial allocation *%DC*			Days-off allocation *%DC*								
							N1			N2			N3		
t	s_1	s_2	s_3	s_1	s_2	s_3	s_1	s_2	s_3	s_1	s_2	s_3	s_1	s_2	s_3
0	100.00	100.00	100.00	44.00	31.11	53.33	16.00	33.33	26.67	44.00	31.11	53.33	12.00	20.00	10.00
1	100.00	100.00	100.00	56.00	35.56	66.67	8.00	26.67	16.67	56.00	35.56	66.67	0.00	2.22	0.00
2	100.00	100.00	100.00	64.00	40.00	56.67	12.00	20.00	23.33	64.00	40.00	56.67	0.00	6.67	6.67
3	100.00	100.00	100.00	56.00	57.78	66.67	16.00	26.67	36.67	56.00	57.78	66.67	0.00	17.78	26.67
4	100.00	100.00	100.00	56.00	82.22	63.33	32.00	33.33	40.00	56.00	82.22	63.33	16.00	33.33	43.33
5	100.00	100.00	100.00	44.00	64.44	53.33	44.00	42.22	50.00	44.00	64.44	53.33	28.00	48.89	56.67
6	100.00	100.00	100.00	44.00	64.44	53.33	64.00	57.78	56.67	44.00	64.44	53.33	48.00	62.22	63.33

Appendix C. Extended numerical results sensitivity analysis days-off scheduling model

In this section, we detail the extended numerical results of the sensibility analysis described in Section 5. We consider the same input data as described in the base case study considering the network N2.

Appendix C.1. Testing strategy

Table C.8 extends the numerical results of the analysis performed in Subsection 5.1.1. We detail the proportion of allocated employees for the different testing strategies: Same rate SR, Incremental rate IR, High rate HR, and no testing. The results are also detailed by employee category. Tables C.9 – C.11 details the results for the performance metrics (see Subsection 3.4), for each value of the evaluated testing rate τ in the sensitivity analysis, considering $\alpha = 8$. Each table corresponds to a different testing strategy, SR, IR, HR, respectively. Recall that $\alpha = 1$ refers to the base scenario values of testing rates (see Table 3). Thus, values above and below the base scenario values indicate and increase or decrease by the factor 0.02. Tables C.9 – C.11 can be used as a guideline with various testing rates to decide upon the expected outcome of the scheduling plan.

Table C.8: Proportion of allocated employees for different testing strategies. network: N2; $\alpha = 8$.

	SR			IR			HR			No testing		
t	s_1	s_2	s_3	s_1	s_2	s_3	s_1	s_2	s_3	s_1	s_2	s_3
0	16.00	31.11	20.00	20.00	31.11	10.00	52.00	68.89	0.00	48.00	60.00	43.33
1	0.00	11.11	6.67	0.00	11.11	3.33	24.00	40.00	0.00	20.00	31.11	26.67
2	4.00	11.11	13.33	0.00	11.11	16.67	12.00	20.00	20.00	8.00	13.33	16.67
3	4.00	17.78	20.00	0.00	17.78	46.67	0.00	8.89	53.33	0.00	4.44	3.33
4	20.00	28.89	30.00	16.00	28.89	66.67	0.00	2.22	70.00	0.00	0.00	0.00
5	32.00	37.78	40.00	28.00	37.78	76.67	0.00	0.00	83.33	0.00	0.00	0.00
6	48.00	51.11	46.67	40.00	51.11	86.67	0.00	0.00	100.00	0.00	0.00	0.00

Table C.9: Sensitivity analysis summary for different testing rates. network: N2; testing strategy: SR; $\alpha = 8$.

τ	%RI	%DC	%DA	%OCC	AL	κ	τ	%RI	%DC	%DA	%OCC	AL	κ	τ	%RI	%DC	%DA	%OCC	AL	κ
0	8.05	56.00	36.67	23.11	1.70	255.33	1.14	11.11	80.00	13.33	48.91	2.51	336.41	2.28	8.04	100.00	3.33	70.32	2.89	439.44
0.02	8.02	56.00	36.67	23.11	1.70	255.67	1.16	10.95	80.00	13.33	48.91	2.51	338.68	2.30	8.01	100.00	0.00	70.56	2.90	440.88
0.04	7.99	56.00	36.67	23.11	1.70	256.00	1.18	11.00	81.00	13.33	49.88	2.53	340.95	2.32	7.99	100.00	0.00	70.56	2.90	441.00
0.06	8.04	56.00	33.33	23.36	1.71	256.47	1.2	11.13	82.00	13.33	50.85	2.55	343.24	2.34	7.99	100.00	0.00	70.56	2.90	441.00
0.08	8.00	56.00	33.33	23.36	1.71	257.00	1.22	11.03	82.00	10.00	51.09	2.56	345.54	2.36	8.00	100.00	0.00	71.05	2.92	441.00
0.1	8.10	56.00	36.67	23.11	1.70	257.56	1.24	10.87	82.00	10.00	51.09	2.56	347.80	2.38	7.97	100.00	0.00	71.29	2.93	441.00
0.12	8.06	56.00	36.67	23.11	1.70	258.15	1.26	10.71	82.00	10.00	51.09	2.56	350.04	2.40	7.98	100.00	0.00	70.56	2.90	441.00
0.14	8.02	56.00	36.67	23.11	1.70	258.74	1.28	10.77	83.00	10.00	52.07	2.58	352.26	2.42	7.99	100.00	0.00	71.53	2.94	441.00
0.16	8.05	56.00	33.33	23.36	1.71	259.35	1.3	10.61	83.00	10.00	52.07	2.58	354.48	2.44	7.92	100.00	0.00	70.80	2.91	441.00
0.18	8.00	56.00	33.33	23.36	1.71	260.00	1.32	10.74	84.00	10.00	53.28	2.61	356.70	2.46	7.92	100.00	0.00	71.53	2.94	441.00
0.2	8.24	57.00	36.67	23.84	1.72	260.68	1.34	10.58	84.00	10.00	53.28	2.61	358.91	2.48	7.97	100.00	0.00	70.56	2.90	441.00
0.22	8.18	57.00	36.67	23.84	1.72	261.48	1.36	10.42	84.00	10.00	53.28	2.61	361.09	2.50	7.93	100.00	0.00	71.78	2.95	441.00
0.24	8.12	57.00	36.67	23.84	1.72	262.38	1.38	10.27	84.00	10.00	53.28	2.61	363.24	2.52	7.99	100.00	0.00	71.78	2.95	441.00
0.26	8.05	57.00	36.67	23.84	1.72	263.31	1.4	10.12	84.00	10.00	53.28	2.61	365.36	2.54	7.99	100.00	0.00	71.29	2.93	441.00
0.28	8.06	57.00	33.33	24.09	1.74	264.21	1.42	9.97	84.00	10.00	53.28	2.61	367.45	2.56	8.00	100.00	0.00	71.78	2.95	441.00
0.3	7.99	57.00	33.33	24.09	1.74	265.00	1.44	10.11	85.00	10.00	54.50	2.64	369.52	2.58	7.51	100.00	0.00	71.53	2.94	441.00
0.32	8.01	58.00	36.67	24.57	1.74	265.89	1.46	9.96	85.00	10.00	54.50	2.64	371.60	2.60	7.82	100.00	0.00	71.78	2.95	441.00
0.34	8.23	58.00	36.67	24.82	1.76	266.80	1.48	9.81	85.00	10.00	54.50	2.64	373.65	2.62	7.82	100.00	0.00	70.80	2.91	441.00
0.36	8.15	58.00	36.67	24.82	1.76	267.83	1.5	9.67	85.00	10.00	54.50	2.64	375.67	2.64	7.11	100.00	0.00	71.05	2.92	441.00
0.38	8.08	58.00	36.67	24.82	1.76	268.87	1.52	9.52	85.00	10.00	54.50	2.64	377.66	2.66	7.55	100.00	0.00	72.26	2.97	441.00
0.4	8.43	59.00	36.67	25.79	1.80	270.05	1.54	9.60	86.00	10.00	55.47	2.65	379.63	2.68	7.91	100.00	0.00	75.18	3.09	441.00
0.42	8.34	59.00	36.67	25.79	1.80	271.22	1.56	9.46	86.00	10.00	55.47	2.65	381.61	2.70	6.03	100.00	0.00	70.56	2.90	441.00
0.44	8.26	59.00	36.67	25.79	1.80	272.43	1.58	9.74	88.00	10.00	57.42	2.68	383.62	2.72	6.00	100.00	0.00	70.56	2.90	441.00
0.46	8.74	61.00	36.67	27.25	1.84	273.70	1.6	9.60	88.00	10.00	57.42	2.68	385.62	2.74	6.00	100.00	0.00	70.56	2.90	441.00
0.48	8.64	61.00	36.67	27.25	1.84	275.08	1.62	9.46	88.00	10.00	57.42	2.68	387.59	2.76	5.99	100.00	0.00	70.80	2.91	441.00
0.5	8.82	62.00	36.67	27.98	1.85	276.46	1.64	9.32	88.00	10.00	57.42	2.68	389.55	2.78	5.99	100.00	0.00	70.56	2.90	441.00
0.52	9.01	63.00	36.67	28.71	1.87	277.88	1.66	9.18	88.00	10.00	57.42	2.68	391.49	2.80	5.98	100.00	0.00	70.56	2.90	441.00
0.54	8.90	63.00	36.67	28.71	1.87	279.37	1.68	9.04	88.00	10.00	57.42	2.68	393.41	2.82	6.00	100.00	0.00	70.56	2.90	441.00
0.56	8.80	63.00	36.67	28.71	1.87	280.83	1.70	8.91	88.00	10.00	57.42	2.68	395.29	2.84	5.99	100.00	0.00	70.56	2.90	441.00
0.58	9.05	64.00	36.67	29.68	1.91	282.33	1.72	8.77	88.00	10.00	57.42	2.68	397.16	2.86	5.97	100.00	0.00	71.53	2.94	441.00
0.6	8.94	64.00	36.67	29.68	1.91	283.90	1.74	8.64	88.00	10.00	57.42	2.68	398.99	2.88	5.98	100.00	0.00	70.56	2.90	441.00
0.62	9.25	65.00	36.67	30.90	1.95	285.50	1.76	8.51	88.00	10.00	57.42	2.68	400.80	2.90	5.99	100.00	0.00	71.29	2.93	441.00
0.64	9.28	65.00	30.00	31.39	1.98	287.14	1.78	8.39	88.00	10.00	57.42	2.68	402.58	2.92	5.99	100.00	0.00	71.53	2.94	441.00
0.66	9.23	65.00	26.67	31.63	2.00	288.77	1.80	8.48	89.00	10.00	58.39	2.70	404.35	2.94	5.98	100.00	0.00	72.51	2.98	441.00
0.68	9.47	66.00	26.67	32.60	2.03	290.49	1.82	8.35	89.00	10.00	58.39	2.70	406.10	2.96	5.69	100.00	0.00	72.26	2.97	441.00
0.7	9.84	67.00	23.33	34.06	2.09	292.25	1.84	8.44	90.00	10.00	59.37	2.71	407.85	2.98	5.97	100.00	0.00	72.51	2.98	441.00
0.72	9.71	67.00	23.33	34.06	2.09	294.09	1.86	8.31	90.00	10.00	59.37	2.71	409.61	3.00	5.89	100.00	0.00	72.51	2.98	441.00
0.74	9.65	67.00	20.00	34.31	2.10	295.92	1.88	8.19	90.00	10.00	59.37	2.71	411.33	3.02	5.86	100.00	0.00	71.53	2.94	441.00
0.76	9.51	67.00	20.00	34.31	2.10	297.80	1.90	8.28	91.00	10.00	60.34	2.73	413.05	3.04	5.77	100.00	0.00	71.29	2.93	441.00
0.78	9.38	67.00	20.00	34.31	2.10	299.66	1.92	8.23	91.00	6.67	60.58	2.74	414.79	3.06	5.53	100.00	0.00	71.29	2.93	441.00
0.8	9.25	67.00	20.00	34.31	2.10	301.53	1.94	8.25	92.00	6.67	61.31	2.74	416.50	3.08	5.90	100.00	0.00	74.94	3.08	441.00
0.82	9.12	67.00	20.00	34.31	2.10	303.39	1.96	8.13	92.00	6.67	61.31	2.74	418.22	3.10	5.93	100.00	0.00	72.26	2.97	441.00
0.84	9.41	68.00	20.00	35.52	2.15	305.22	1.98	8.01	92.00	6.67	61.31	2.74	419.92	3.12	5.98	100.00	0.00	75.67	3.11	441.00
0.86	9.56	69.00	20.00	36.50	2.17	307.12	2.00	8.11	93.00	6.67	62.53	2.76	421.50	3.14	5.72	100.00	0.00	72.99	3.00	441.00
0.88	9.71	70.00	20.00	37.47	2.20	309.03	2.02	8.06	94.00	10.00	63.02	2.76	423.11	3.16	5.21	100.00	0.00	71.29	2.93	441.00
0.9	9.57	70.00	20.00	37.47	2.20	310.97	2.04	8.09	94.00	6.67	63.50	2.78	424.79	3.18	5.57	100.00	0.00	71.29	2.93	441.00
0.92	9.44	70.00	20.00	37.47	2.20	312.89	2.06	8.04	95.00	10.00	63.99	2.77	426.37	3.20	5.36	100.00	0.00	73.24	3.01	441.00
0.94	9.66	71.00	20.00	38.69	2.24	314.81	2.08	8.00	95.00	6.67	64.23	2.78	427.93	3.22	5.29	100.00	0.00	72.75	2.99	441.00
0.96	9.52	71.00	20.00	38.69	2.24	316.76	2.10	8.05	95.00	0.00	64.72	2.80	429.31	3.24	4.02	100.00	0.00	70.56	2.90	441.00
0.98	10.09	73.00	20.00	41.12	2.32	318.72	2.12	8.03	96.00	3.33	65.45	2.80	430.62	3.26	3.99	100.00	0.00	70.56	2.90	441.00
1	9.95	73.00	20.00	41.12	2.32	320.77	2.14	7.99	96.00	0.00	65.69	2.81	432.00	3.28	3.99	100.00	0.00	70.56	2.90	441.00
1.02	10.23	74.00	16.67	42.58	2.36	322.80	2.16	8.06	97.00	3.33	66.67	2.82	433.17	3.30	3.98	100.00	0.00	70.80	2.91	441.00
1.04	10.72	76.00	16.67	44.77	2.42	324.91	2.18	8.03	97.00	0.00	66.91	2.84	434.63	3.32	3.98	100.00	0.00	70.56	2.90	441.00
1.06	11.21	78.00	13.33	46.96	2.47	327.11	2.20	8.03	98.00	3.33	67.88	2.85	435.62	3.34	3.99	100.00	0.00	70.56	2.90	441.00
1.08	11.32	79.00	13.33	47.93	2.49	329.46	2.22	8.00	98.00	0.00	68.13	2.86	437.00	3.36	3.89	100.00	0.00	70.80	2.91	441.00
1.1	11.16	79.00	13.33	47.93	2.49	331.79	2.24	8.02	99.00	3.33	69.10	2.87	437.75	3.38	4.00	100.00	0.00	71.29	2.93	441.00
1.12	11.28	80.00	13.33	48.91	2.51	334.11	2.26	8.00	99.00	0.00	69.34	2.88	439.00	3.40	3.99	100.00	0.00	71.53	2.94	441.00

Table C.10: Sensitivity analysis summary for different testing rates. network: N2; testing strategy: IR; $\alpha = 8$.

τ	%RI	%DC	%DA	%OCC	AL	κ	τ	%RI	%DC	%DA	%OCC	AL	κ	τ	%RI	%DC	%DA	%OCC	AL	κ
0	8.05	56.00	36.67	23.11	1.70	255.33	1.02	10.18	81.00	20.00	49.39	2.51	345.41	2.04	8.01	98.00	0.00	68.13	2.86	436.92
0.02	8.02	56.00	36.67	23.11	1.70	255.68	1.04	10.08	81.00	16.67	49.64	2.52	347.93	2.06	7.95	98.00	0.00	68.13	2.86	437.00
0.04	8.00	56.00	36.67	23.11	1.70	256.00	1.06	9.90	81.00	16.67	49.64	2.52	350.40	2.08	8.00	99.00	3.33	69.10	2.87	438.00
0.06	8.05	56.00	33.33	23.36	1.71	256.37	1.08	9.73	81.00	16.67	49.64	2.52	352.82	2.1	7.98	99.00	0.00	69.34	2.88	439.00
0.08	8.01	56.00	33.33	23.36	1.71	256.88	1.1	9.84	82.00	16.67	50.61	2.54	355.24	2.12	7.96	99.00	0.00	69.59	2.89	439.00
0.1	8.11	56.00	36.67	23.11	1.70	257.52	1.12	9.67	82.00	16.67	50.61	2.54	357.63	2.14	8.00	100.00	3.33	70.32	2.89	440.00
0.12	8.06	56.00	36.67	23.11	1.70	258.21	1.14	9.79	83.00	16.67	51.58	2.55	359.98	2.16	8.00	100.00	0.00	70.56	2.90	441.00
0.14	8.00	56.00	36.67	23.11	1.70	258.96	1.16	9.69	83.00	13.33	51.82	2.57	362.34	2.18	7.99	100.00	0.00	70.56	2.90	441.00
0.16	8.02	56.00	33.33	23.36	1.71	259.72	1.18	9.52	83.00	13.33	51.82	2.57	364.67	2.2	7.98	100.00	0.00	70.56	2.90	441.00
0.18	8.26	57.00	36.67	23.84	1.72	260.38	1.2	9.36	83.00	13.33	51.82	2.57	366.96	2.22	7.97	100.00	0.00	70.56	2.90	441.00
0.2	8.19	57.00	36.67	23.84	1.72	261.27	1.22	9.27	83.00	10.00	52.07	2.58	369.21	2.24	8.00	100.00	0.00	71.05	2.92	441.00
0.22	8.13	57.00	36.67	23.84	1.72	262.20	1.24	9.11	83.00	10.00	52.07	2.58	371.45	2.26	7.99	100.00	0.00	70.56	2.90	441.00
0.24	8.48	58.00	36.67	24.82	1.76	263.23	1.26	8.95	83.00	10.00	52.07	2.58	373.64	2.28	7.96	100.00	0.00	70.56	2.90	441.00
0.26	8.40	58.00	36.67	24.82	1.76	264.41	1.28	8.80	83.00	10.00	52.07	2.58	375.80	2.3	8.00	100.00	0.00	71.53	2.94	441.00
0.28	8.31	58.00	36.67	24.82	1.76	265.65	1.3	8.65	83.00	10.00	52.07	2.58	377.91	2.32	7.84	100.00	0.00	71.78	2.95	441.00
0.3	8.22	58.00	36.67	24.82	1.76	266.95	1.32	8.64	84.00	13.33	53.04	2.60	380.00	2.34	7.97	100.00	0.00	70.56	2.90	441.00
0.32	8.12	58.00	36.67	24.82	1.76	268.25	1.34	8.49	84.00	13.33	53.04	2.60	382.07	2.36	7.82	100.00	0.00	72.26	2.97	441.00
0.34	8.03	58.00	36.67	24.82	1.76	269.55	1.36	8.35	84.00	13.33	53.04	2.60	384.11	2.38	7.94	100.00	0.00	70.56	2.90	441.00
0.36	8.29	59.00	36.67	25.79	1.80	270.97	1.38	8.49	85.00	13.33	54.26	2.62	386.14	2.4	7.94	100.00	0.00	71.53	2.94	441.00
0.38	8.68	60.00	33.33	27.01	1.85	272.49	1.4	8.35	85.00	13.33	54.26	2.62	388.14	2.42	7.56	100.00	0.00	71.29	2.93	441.00
0.4	8.57	60.00	33.33	27.01	1.85	274.09	1.42	8.63	86.00	10.00	55.72	2.66	390.15	2.44	7.76	100.00	0.00	71.53	2.94	441.00
0.42	8.45	60.00	33.33	27.01	1.85	275.70	1.44	8.49	86.00	10.00	55.72	2.66	392.14	2.46	7.37	100.00	0.00	70.56	2.90	441.00
0.44	8.34	60.00	33.33	27.01	1.85	277.29	1.46	8.35	86.00	10.00	55.72	2.66	394.09	2.48	7.98	100.00	0.00	76.16	3.13	441.00
0.46	8.79	62.00	33.33	28.47	1.89	278.93	1.48	8.21	86.00	10.00	55.72	2.66	396.01	2.5	7.91	100.00	0.00	70.80	2.91	441.00
0.48	8.67	62.00	33.33	28.47	1.89	280.63	1.5	8.08	86.00	10.00	55.72	2.66	397.91	2.52	7.98	100.00	0.00	77.86	3.20	441.00
0.5	8.55	62.00	33.33	28.47	1.89	282.35	1.52	8.30	87.00	10.00	56.93	2.69	399.77	2.54	7.94	100.00	0.00	75.91	3.12	441.00
0.52	8.85	63.00	33.33	29.68	1.94	284.07	1.54	8.17	87.00	10.00	56.93	2.69	401.65	2.56	6.02	100.00	0.00	70.56	2.90	441.00
0.54	9.01	64.00	33.33	30.66	1.97	285.89	1.56	8.04	87.00	10.00	56.93	2.69	403.50	2.58	5.99	100.00	0.00	70.56	2.90	441.00
0.56	8.88	64.00	33.33	30.66	1.97	287.75	1.58	8.20	88.00	10.00	57.91	2.70	405.23	2.6	5.99	100.00	0.00	70.56	2.90	441.00
0.58	8.74	64.00	33.33	30.66	1.97	289.57	1.6	8.07	88.00	10.00	57.91	2.70	407.05	2.62	5.99	100.00	0.00	70.56	2.90	441.00
0.6	8.97	65.00	33.33	31.87	2.02	291.44	1.62	8.02	89.00	13.33	58.39	2.70	408.73	2.64	5.93	100.00	0.00	70.80	2.91	441.00
0.62	9.33	66.00	30.00	33.33	2.08	293.41	1.64	8.12	89.00	10.00	58.88	2.72	410.32	2.66	5.98	100.00	0.00	70.56	2.90	441.00
0.64	9.54	67.00	26.67	34.55	2.12	295.43	1.66	8.00	89.00	10.00	58.88	2.72	412.00	2.68	5.93	100.00	0.00	70.56	2.90	441.00
0.66	10.31	70.00	26.67	37.47	2.20	297.66	1.68	8.03	90.00	10.00	59.61	2.72	413.63	2.7	5.93	100.00	0.00	71.53	2.94	441.00
0.68	10.64	72.00	30.00	39.17	2.24	300.06	1.7	8.06	90.00	6.67	60.10	2.74	415.18	2.72	5.97	100.00	0.00	71.78	2.95	441.00
0.7	11.32	74.00	23.33	41.61	2.31	302.58	1.72	8.01	91.00	10.00	60.58	2.74	416.82	2.74	5.99	100.00	0.00	71.29	2.93	441.00
0.72	11.13	74.00	23.33	41.61	2.31	305.20	1.74	8.05	92.00	10.00	61.31	2.74	418.30	2.76	5.95	100.00	0.00	71.29	2.93	441.00
0.74	11.16	75.00	23.33	42.58	2.33	307.81	1.76	8.01	92.00	10.00	61.56	2.75	419.89	2.78	6.00	100.00	0.00	70.80	2.91	441.00
0.76	10.96	75.00	23.33	42.58	2.33	310.49	1.78	8.04	93.00	10.00	62.29	2.75	421.39	2.8	5.98	100.00	0.00	72.26	2.97	441.00
0.78	10.85	75.00	20.00	42.82	2.35	313.16	1.8	8.01	93.00	6.67	62.53	2.76	422.92	2.82	5.94	100.00	0.00	70.80	2.91	441.00
0.8	11.08	77.00	23.33	44.77	2.39	315.88	1.82	8.06	94.00	6.67	63.75	2.79	425.18	2.84	5.97	100.00	0.00	71.29	2.93	441.00
0.82	10.89	77.00	23.33	44.77	2.39	318.61	1.84	8.01	94.00	6.67	63.75	2.79	425.82	2.86	6.00	100.00	0.00	72.51	2.98	441.00
0.84	10.69	77.00	23.33	44.77	2.39	321.28	1.86	7.99	94.00	6.67	63.75	2.79	426.00	2.88	5.99	100.00	0.00	70.80	2.91	441.00
0.86	11.07	79.00	23.33	46.96	2.44	323.97	1.88	8.04	95.00	3.33	64.72	2.80	428.39	2.9	5.99	100.00	0.00	72.75	2.99	441.00
0.88	11.02	79.00	16.67	47.45	2.47	326.71	1.9	8.02	95.00	0.00	64.96	2.81	429.76	2.92	5.63	100.00	0.00	71.05	2.92	441.00
0.9	10.97	80.00	20.00	48.18	2.48	329.48	1.92	7.99	96.00	6.67	65.45	2.80	431.00	2.94	5.70	100.00	0.00	71.53	2.94	441.00
0.92	10.77	80.00	20.00	48.18	2.48	332.20	1.94	8.05	96.00	0.00	65.94	2.82	432.29	2.96	5.76	100.00	0.00	70.80	2.91	441.00
0.94	10.94	81.00	20.00	49.39	2.51	334.90	1.96	7.99	96.00	0.00	65.94	2.82	433.00	2.98	5.05	100.00	0.00	72.75	2.99	441.00
0.96	10.74	81.00	20.00	49.39	2.51	337.59	1.98	8.07	97.00	0.00	66.91	2.84	434.09	3	5.34	100.00	0.00	71.53	2.94	441.00
0.98	10.55	81.00	20.00	49.39	2.51	340.25	2	7.96	97.00	0.00	66.91	2.84	435.00							
1	10.37	81.00	20.00	49.39	2.51	342.86	2.02	8.03	98.00	3.33	67.88	2.85	435.62							

Table C.11: Sensitivity analysis summary for different testing rates. network: N2; testing strategy: HR; $\alpha = 8$.

τ	$\%RI$	$\%DC$	$\%DA$	$\%OCC$	AL	κ	τ	$\%RI$	$\%DC$	$\%DA$	$\%OCC$	AL	κ
0	8.05	56.00	36.67	23.11	1.70	255.33	0.58	8.00	73.00	26.67	41.36	2.33	333.00
0.02	8.02	56.00	36.67	23.11	1.70	255.71	0.6	8.05	74.00	26.67	42.09	2.34	334.36
0.04	8.20	56.00	36.67	23.11	1.70	256.18	0.62	8.02	74.00	23.33	42.34	2.35	335.74
0.06	8.13	56.00	36.67	23.11	1.70	257.21	0.64	8.01	74.00	20.00	42.58	2.36	336.85
0.08	8.11	56.00	36.67	23.36	1.71	258.53	0.66	8.01	74.00	23.33	42.82	2.38	337.82
0.1	8.04	56.00	33.33	23.60	1.73	260.45	0.68	8.00	74.00	26.67	42.58	2.36	338.95
0.12	8.17	57.00	36.67	24.33	1.75	262.60	0.7	8.01	75.00	30.00	43.07	2.36	339.92
0.14	8.06	57.00	33.33	24.57	1.77	265.12	0.72	8.02	75.00	26.67	43.31	2.37	340.79
0.16	8.25	58.00	33.33	25.30	1.79	267.52	0.74	8.03	75.00	23.33	43.55	2.39	341.57
0.18	8.41	59.00	33.33	26.76	1.86	270.31	0.76	8.06	75.00	20.00	43.80	2.40	342.15
0.2	8.55	60.00	33.33	27.98	1.92	273.31	0.78	8.00	75.00	20.00	43.80	2.40	342.94
0.22	8.95	62.00	30.00	30.17	2.00	276.74	0.8	8.05	76.00	26.67	44.28	2.39	343.35
0.24	9.23	64.00	30.00	32.36	2.08	280.84	0.82	8.00	76.00	30.00	43.80	2.37	344.00
0.26	9.15	65.00	30.00	33.33	2.11	284.95	0.84	8.04	76.00	26.67	44.04	2.37	344.48
0.28	9.27	67.00	33.33	35.28	2.16	289.25	0.86	8.00	75.00	20.00	43.80	2.40	345.00
0.3	9.46	69.00	33.33	37.47	2.23	293.58	0.88	8.04	76.00	23.33	44.28	2.39	345.45
0.32	9.15	69.00	33.33	37.47	2.23	297.84	0.9	8.00	76.00	23.33	44.28	2.39	345.93
0.34	8.87	69.00	33.33	37.47	2.23	301.80	0.92	8.06	76.00	20.00	44.53	2.41	346.09
0.36	8.68	69.00	30.00	37.71	2.25	305.49	0.94	8.04	76.00	20.00	44.53	2.41	346.51
0.38	8.43	69.00	30.00	37.71	2.25	308.99	0.96	8.01	76.00	20.00	44.53	2.41	346.88
0.4	8.19	69.00	30.00	37.71	2.25	312.28	0.98	7.98	76.00	20.00	44.53	2.41	347.00
0.42	8.11	70.00	33.33	38.69	2.27	315.42	1	8.05	76.00	23.33	44.53	2.41	347.24
0.44	8.05	70.00	26.67	39.17	2.30	318.30	1.02	8.03	76.00	23.33	44.53	2.41	347.54
0.46	8.07	71.00	33.33	39.42	2.28	321.00	1.04	8.01	76.00	23.33	44.53	2.41	347.82
0.48	8.03	71.00	26.67	39.90	2.31	323.52	1.06	7.99	76.00	23.33	44.53	2.41	348.00
0.5	8.03	72.00	26.67	40.63	2.32	325.63	1.08	8.07	76.00	20.00	44.77	2.42	348.02
0.52	8.02	72.00	30.00	40.39	2.31	327.74	1.1	8.05	76.00	20.00	44.77	2.42	348.24
0.54	8.02	73.00	30.00	41.12	2.32	329.65	1.12	8.04	76.00	20.00	44.77	2.42	348.44
0.56	8.05	73.00	23.33	41.61	2.34	331.29							

Appendix C.2. Threshold on allocation decisions and risk of infection

Tables C.12 and C.13 summarize the results of the sensitivity analysis over the threshold of the expected number of infected employees, α, analyzed in Subsection 5.1.2. Table C.12 details the proportion of infected employees for several values of α and testing strategies. Table C.13 shows the expected proportion of allocated employees. Each panel considers different testing rates for the testing strategies. The first panel considers τ : SR = 5%, IR = 1%, 5%, 18%, HR = 75%; The second panel considers τ : SR = 20%, IR = 15%, 20%, 33%, HR = 100%; The third panel considers τ : SR = 35%, IR = 30%, 35%, 48%, HR = 100%.

Table C.12: Expected proportion of infected employees, *RI*, for several values of α and testing strategies.

α	τ : SR=5%, IR=1%, 5%, 18%, HR=75%				τ : SR=20%, IR=15%, 20%, 33%, HR=100%				τ : SR=35%, IR=30%, 35%, 48%, HR=100%			
	SR	IR	HR	No testing	SR	IR	HR	No testing	SR	IR	HR	No testing
0	7.56	8.40	7.88	7.16	9.95	10.37	5.63	7.16	8.35	7.10	5.63	7.16
2	7.56	8.40	7.88	7.16	9.95	10.37	5.63	7.16	8.35	7.10	5.63	7.16
4	7.56	8.40	7.88	7.16	9.95	10.37	5.63	7.16	8.35	7.10	5.63	7.16
6	7.56	8.40	7.88	7.16	9.95	10.37	6.06	7.16	8.35	7.10	6.06	7.16
8	8.00	8.40	8.25	8.05	9.95	10.37	8.05	8.05	8.35	8.01	8.05	8.05
10	10.06	10.05	10.01	10.07	10.02	10.37	10.00	10.07	10.03	10.07	10.00	10.07
12	12.04	12.04	12.01	12.03	12.00	12.02	12.05	12.03	11.98	11.01	12.05	12.03
14	14.07	14.01	14.00	14.04	14.07	14.01	13.95	14.04	11.98	11.01	13.95	14.04
16	16.04	16.04	15.98	16.04	16.01	16.03	15.97	16.04	11.98	11.01	15.97	16.04
18	17.97	18.01	17.96	17.96	18.03	17.99	18.03	17.96	11.98	11.01	18.03	17.96
20	20.00	20.05	20.00	20.04	19.97	17.99	19.97	20.04	11.98	11.01	19.97	20.04

Table C.13: Expected proportion of allocated employees for several values of α and testing strategies.

α	τ : SR=5%, IR=1%, 5%, 18%, HR=75%				τ : SR=20%, IR=15%, 20%, 33%, HR=100%				τ : SR=35%, IR=30%, 35%, 48%, HR=100%			
	SR	IR	HR	No testing	SR	IR	HR	No testing	SR	IR	HR	No testing
0	55.00	58.00	57.00	53.00	73.00	81.00	70.00	53.00	89.00	88.00	70.00	53.00
2	55.00	58.00	57.00	53.00	73.00	81.00	70.00	53.00	89.00	88.00	70.00	53.00
4	55.00	58.00	57.00	53.00	73.00	81.00	70.00	53.00	89.00	88.00	70.00	53.00
6	55.00	58.00	57.00	53.00	73.00	81.00	71.00	53.00	89.00	88.00	71.00	53.00
8	56.00	58.00	58.00	56.00	73.00	81.00	76.00	56.00	89.00	92.00	76.00	56.00
10	62.00	62.00	63.00	60.00	73.00	81.00	81.00	60.00	96.00	99.00	81.00	60.00
12	66.00	67.00	68.00	65.00	79.00	86.00	86.00	65.00	100.00	100.00	86.00	65.00
14	71.00	72.00	73.00	69.00	86.00	91.00	89.00	69.00	100.00	100.00	89.00	69.00
16	75.00	77.00	78.00	73.00	92.00	97.00	92.00	73.00	100.00	100.00	92.00	73.00
18	78.00	80.00	82.00	77.00	98.00	100.00	96.00	77.00	100.00	100.00	96.00	77.00
20	82.00	84.00	86.00	80.00	100.00	100.00	99.00	80.00	100.00	100.00	99.00	80.00

Appendix C.3. Workload demand configuration

Table C.14 details the proportion of allocated employees for different settings of the workload demand as described in Subsection 5.2. We define the required number of employees per setting as follows: Setting 1: $s_1 = 25$, $s_2 = 45$, $s_3 = 30$; Setting 2: $s_1 = 34$, $s_2 = 33$, $s_3 = 33$; Setting 3: $s_1 = 30$ $s_2 = 25$ $s_3 = 45$.

Table C.14: Proportion of allocated employees for different workload demand configurations.

	Setting 1			Setting 2			Setting 3		
	Demand coverage (%DC)								
t	s_1	s_2	s_3	s_1	s_2	s_3	s_1	s_2	s_3
0	16.00	31.11	20.00	14.71	18.18	12.12	10.00	12.00	17.78
1	0.00	11.11	6.67	0.00	0.00	0.00	0.00	0.00	0.00
2	4.00	11.11	13.33	0.00	9.09	6.06	3.33	8.00	6.67
3	4.00	17.78	20.00	2.94	21.21	24.24	6.67	20.00	24.44
4	20.00	28.89	30.00	17.65	39.39	39.39	20.00	36.00	37.78
5	32.00	37.78	40.00	29.41	54.55	51.52	33.33	60.00	48.89
6	48.00	51.11	46.67	47.06	72.73	57.58	53.33	72.00	55.56